Summary of presentation:
disruption mitigation using shattered pellet injection

IAEA technical meeting on plasma disruptions and their mitigation

2020. 07. 22

Jayhyun Kim

on behalf of the speakers in Mitigation_SPI session

Classification of topics (total 17 talks in the session)

- ITER DMS strategy and its activities
  - 128. Session Introduction: Disruption Mitigation by Shattered Pellet Injection by Nicholas Eidietis (General Atomics)
  - 154. The ITER Disruption Mitigation Strategy by Michael Lehnen (ITER Organization)

  - 101. Mitigation of disruption electro-magnetic load with SPI on JET-ILW by Sergei Gerasimov (CCFE)
  - 116. Disruption mitigation by multiple injection of shattered pellets in KSTAR by Jayhyun Kim (NFRI)
  - 135. ASDEX Upgrade SPI: design, status and plans by Gergely Papp (IPP, Garching)
  - 140. Overview of the Radiated Fraction and Radiation Asymmetries Following Shattered Pellet Injection by Ryan Sweeney (Massachusetts Institute of Technology)

  - 111. Progress on non-linear MHD simulations of ITER Shattered Pellet Injection by Di Hu (Beihang University)
  - 142. Verification and Validation of Extended-Magnetohydrodynamic Modeling of Disruption Mitigation by Brendan C. Lyons (General Atomics)

- Injection schemes of SPI (especially for RE mitigation)
  - 106. DIII-D Exploration of the D2+Kink Path to Runaway Electron Mitigation in Tokamaks by Carlos Paz-Soldan (General Atomics)
  - 132. Mitigation of runaway electron heat loads by deuterium SPI injection and kink activity by Cedric Reux (CEA)
  - 136. Non-linear simulation of benign RE beam termination in JET D2 second-injection experiment by Vinodh Kumar Bandaru (IPP, Garching)

  - 131. On the possible injection schemes with the ITER SPI system by Eric Nardon (CEA)

- Pellet/shards dynamics: shattering, ablation/sublimation, assimilation
  - 127. Shatter Plume Analysis from the JET, KSTAR, and DIII-D Shattered Pellet Injectors by Trey Gebhart (Oak Ridge National Laboratory)
  - 151. Near-field models and simulation of the ablation of pellets and SPI fragments for plasma disruption mitigation in tokamaks by Roman Samulyak (*Stony Brook Univ.)*
  - 148. Pellet sublimation and expansion under runaway electron flux by Dmitrii I. Kiramov (National Research Centre Kurchatov Institute)

  - 117. Particle Assimilation During Shattered Pellet Injection by Daisuke Shiraki (Oak Ridge National Laboratory)
  - 134. Study of the companion plasma during runaway electron mitigation experiments with massive material injection in the JET tokamak by Sundaresan Sridhar (CEA)

ITER DMS strategy and its activities

- Introduction
  - 128. Session Introduction: Disruption Mitigation by Shattered Pellet Injection
  - 154. The ITER Disruption Mitigation Strategy

- Experiments with including its preparation
  - 101. Mitigation of disruption electro-magnetic load with SPI on JET-ILW
  - 116. Disruption mitigation by multiple injection of shattered pellets in KSTAR
  - 135. ASDEX Upgrade SPI: design, status and plans
  - 140. Overview of the Radiated Fraction and Radiation Asymmetries Following Shattered Pellet Injection

- Numerical simulation/modeling with its verification and validation
  - 111. Progress on non-linear MHD simulations of ITER Shattered Pellet Injection
  - 142. Verification and Validation of Extended-Magnetohydrodynamic Modeling of Disruption Mitigation

Worldwide SPI research program has increased dramatically in recent years to meet near-term research needs of ITER DMS

Experimental explosion since 2018…

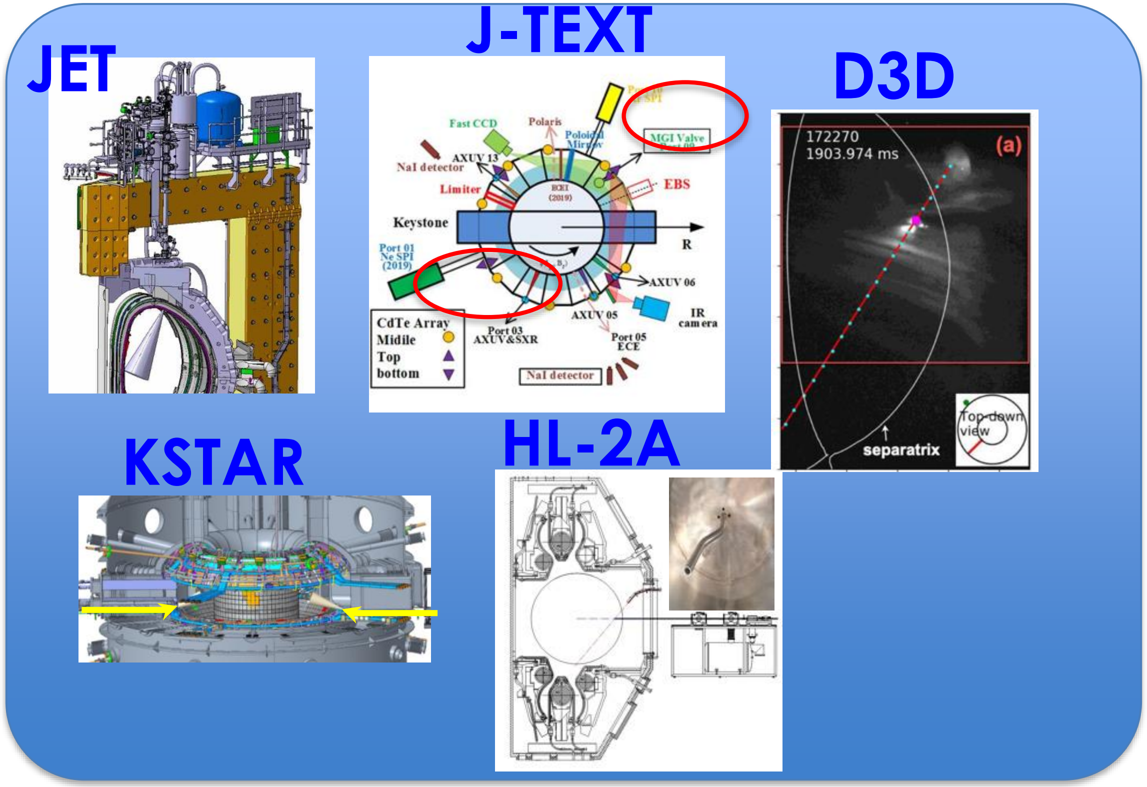

Rapidly increasing theory & modeling effort

JOREK, NIMROD, M3D-C1 Modeling of ITER/JET/KSTAR/D3D SPI Scenarios

Basic SPI ablation modeling

+ Massive RE modeling effort

New organizational structures to facilitate & coordinate SPI research

ITER Disruption Task Force

ITPA MDC-24 "SPI Physics Validation"

154 - M. Lehnen: The ITER Disruption Mitigation Strategy

- The **ITER DMS** can inject 24 pellets (28.5x57mm) from 3 equatorial ports and 3 pellets from 3 upper ports, final design is expected in 2022
- **Key design input required:** a) jitter in fragment arrival time, b) fragment velocity dispersion, c) fragment size and velocity
- **DMS reaction time** (relevant for trigger development) depends mainly on pellet flight time (Ne/Ar: 30-40ms, H: 10ms)
- The **DMS Requirements** (injection species and quantities) were defined on present knowledge, large uncertainties for some and validation/revision is part of the DMS TF work:
  - Thermal load mitigation to keep thermal energy conducted to the first wall and divertor below 20 MJ, to avoid first wall melting from radiation peaking or from magnetic energy deposition, to avoid runaway electron formation
  - RE impact mitigation through high-Z or hydrogen injection?
  - Current quench control to keep $50 < t_{CQ} < 150$ ms
- **DMS TF activities:**
  - Theory& Modelling to address runaway electrons and perform 3D SPI modelling
  - Experiments: KSTAR to address efficiency of multiple injection with 2 injection locations (density rise, radiation distribution) / ASDEX to identify the optimum fragment size and velocity
  - Technology: Development of key components (e.g. pellet diagnostic) and optimisation of pellet forming, launching and shattering

S. Gerasimov. Mitigation of disruption electromagnetic load with SPI

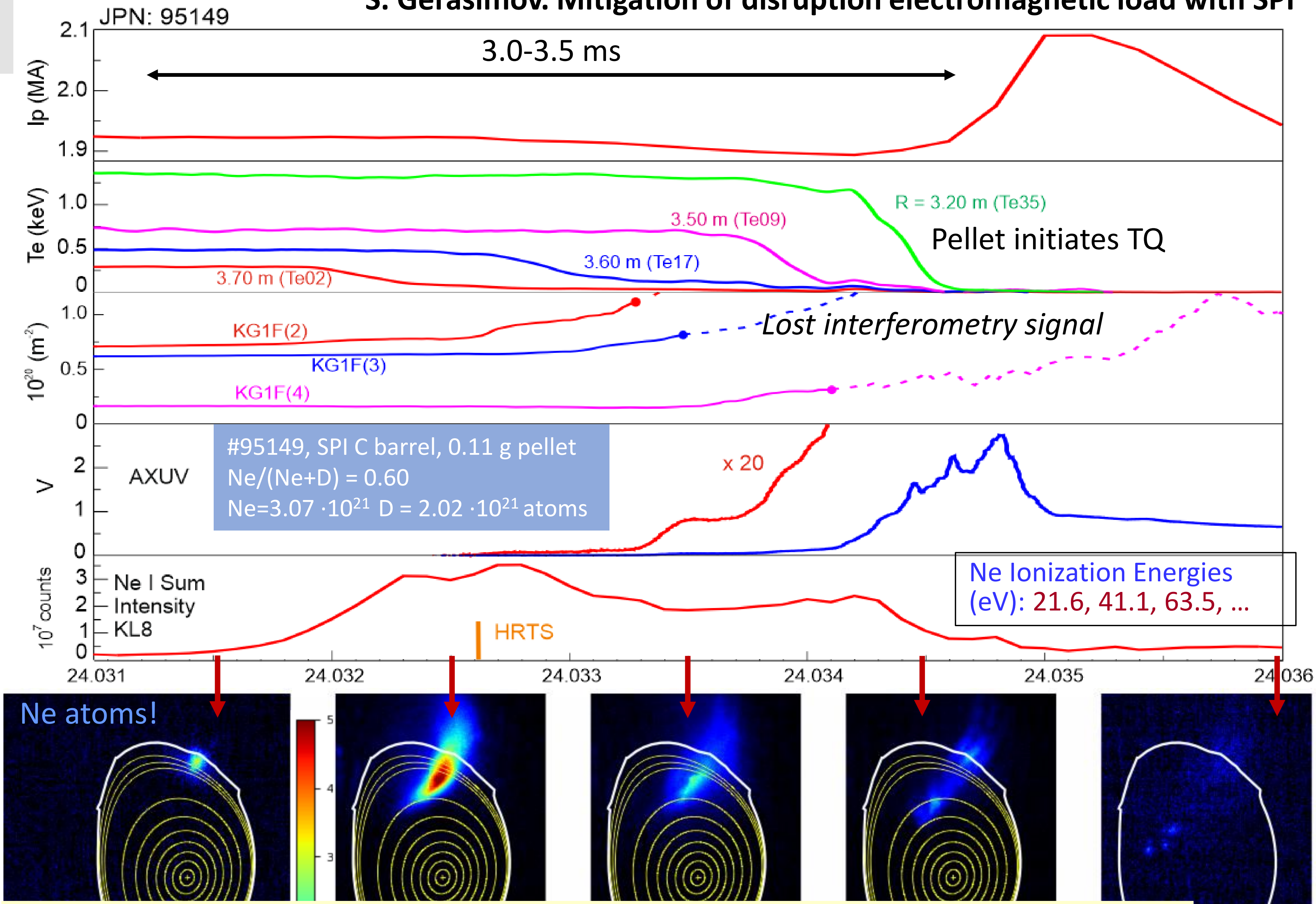

Small pellet (Ne neutrals) is assimilated during cooling, TQ and MHD phases

JET

S. Gerasimov. Mitigation of disruption electromagnetic load with SPI

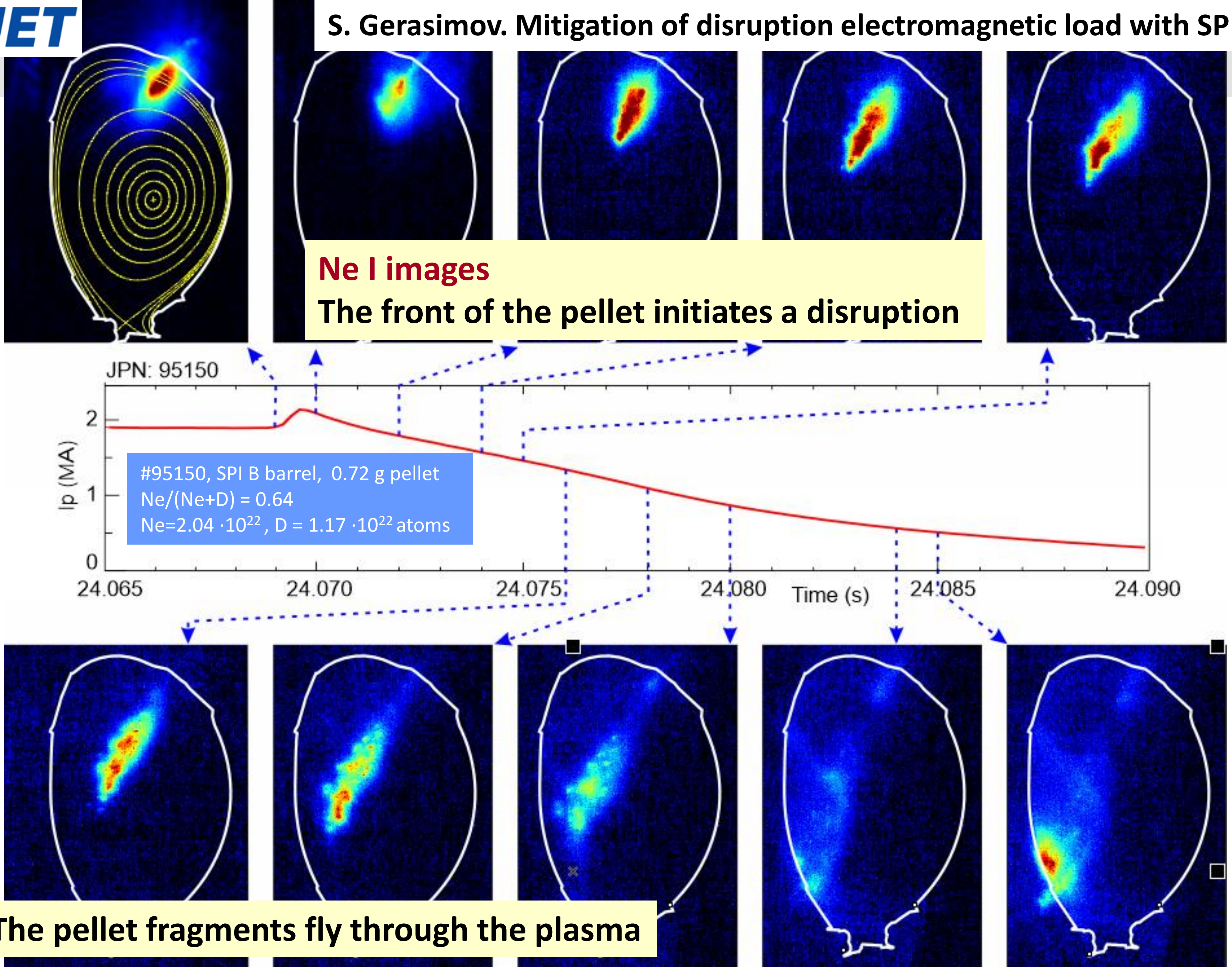

3D Ar^{-1} observed Plasma Helical Streams, can be used to calibrate the models

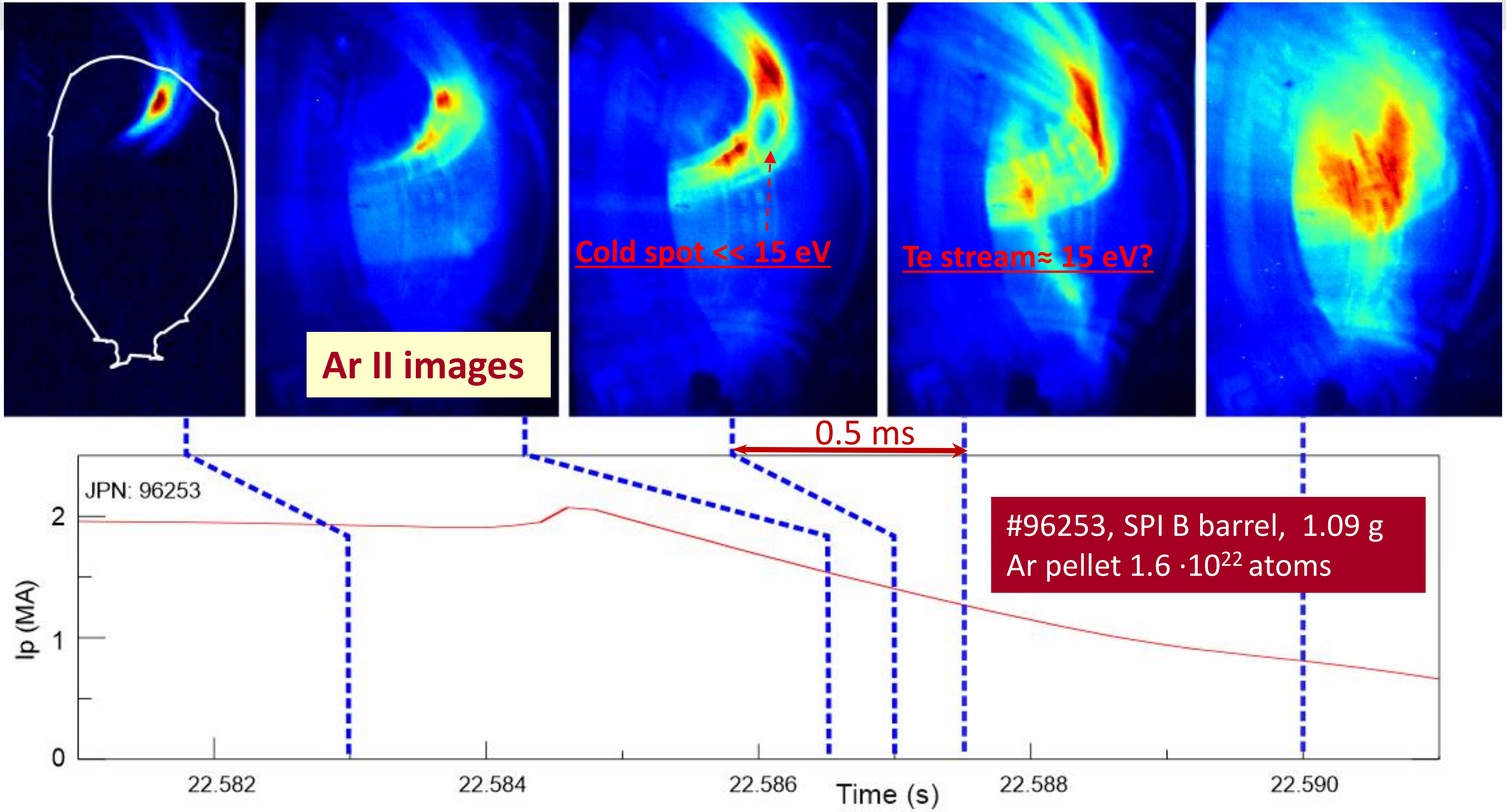

Plasma travels along magnetic field with ion sound speed $v_s = \sqrt{\frac{T_e}{m_i}}$

Ar Ionization Energies (eV): 15.8, 27.6, 40.9, 59.8, 75, 91.3, 123.3, 143.9, 422.6, 479 …..

Summary

- There is a marginal effect of pellet integrity on CQ duration
- Strong dependence of CQ duration on Ne fraction
- There is a marginal effect of pellet size on CQ duration
- SPI effectiveness ($\tau_{80\text{-}20}$) does not depend on pre-disruptive Ip for B pellet
  - ✓ *may be some dependence for C pellet*
- SPI prevents AVDE, similar to MGI effect
- SPI effectiveness ($\tau_{80\text{-}20}$) does not depend on plasma status:
  - ✓ normal ("healthy") i.e., not prone to disruption
  - ✓ post-disruptive plasma *(only one pulse was done!)*
  - ✓ *off-normal (affected by LM) pre-disruptive plasma has not been tested yet*

Summary - implications for ITER

- The JET-ILW study on SPI provided vast experimental data including plasma characterisation for various SPI:
  - Pellet cloud dimension and speed;
  - Pellet assimilated and ionisation during cooling, TQ, MHD and CQ phases;
  - Plasma density temporal evaluation including CQ;
  - ECE cut-off observed during TQ even for smallest pellet, it suggests excising of high density blooms;
  - Clear unique observation of cold 3D Ar plasma helical streams
- The study provided massive experimental data on effect of SPI on mitigation of disruption electromagnetic loads:
  - Strong dependence of CQ duration on Ne fraction;
  - There is a marginal effect of pellet size on CQ duration;
  - SPI effectiveness on pre-disruptive Ip;
  - It was demonstrated that SPI is effective tool to prevent AVDE;
  - Fist experiments suggest that SPI effectiveness does not depend on plasma status
- This presentation includes careful description of the used diagnostics and possible issues with data interpretation with aim to implement synthetic diagnostics in numerical models
- JET-ILW unique experimental data that can help to improve the understanding of disruptions and to develop and to calibrate numerical models, which could be used to predict the loads with future machines, such as ITER

Dual SPIs made higher density during disruption mitigation in KSTAR
→ promising result in relation with ITER DMS strategy against RE suppression.

- New dispersion interferometer measured the abrupt density rise.
  - It uses short wavelength (1064 nm) for avoiding density cutoff and refraction.
  - Conventional two color interferometer suffered fringe jump during disruption mitigation.

Nearly double density by dual SPIs

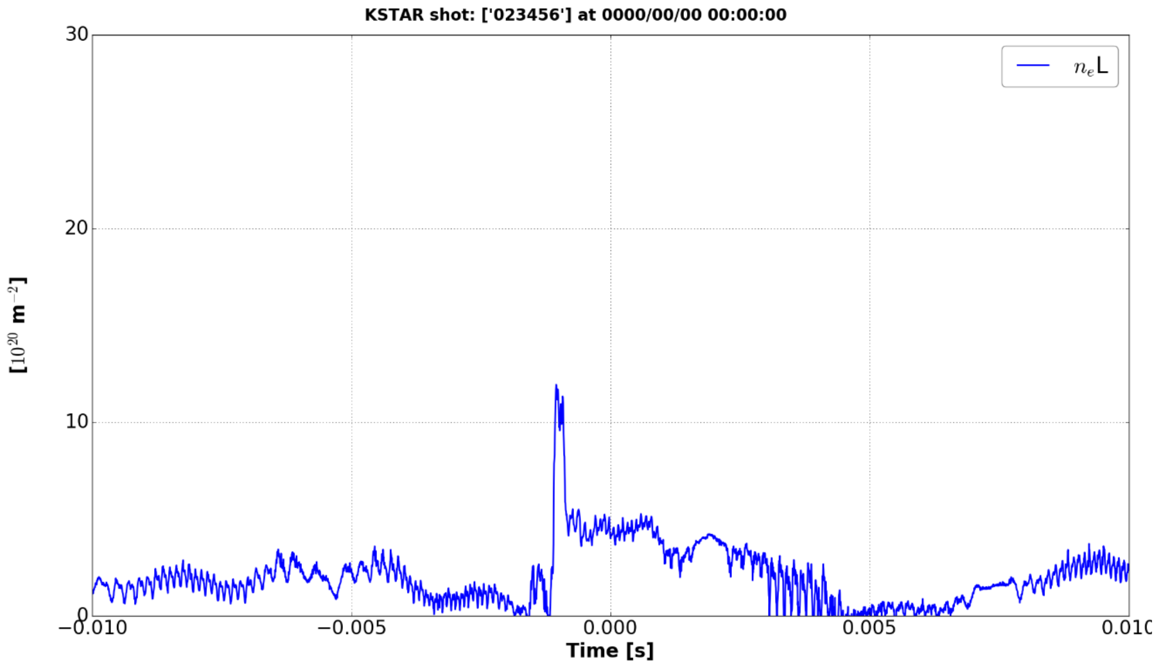

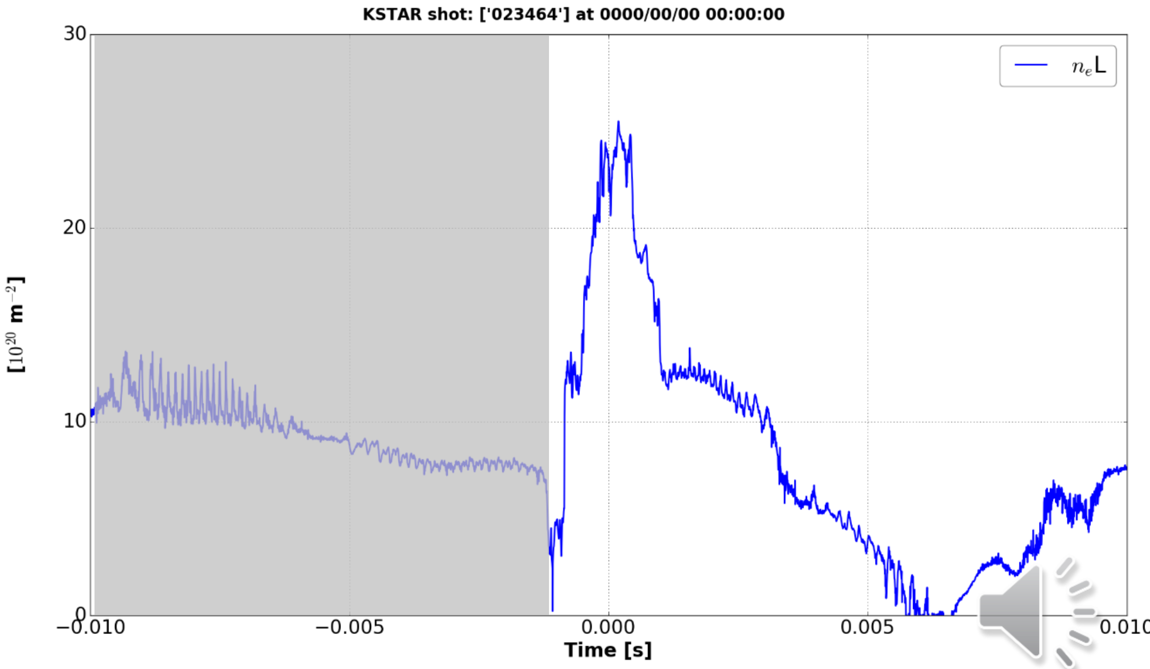

Intentional asynchronization of dual SPIs exhibited slower current quench in proportion to the time delay between two SPIs in KSTAR

- Even within thermal quench duration, the delay level affected the quench rate.
- We measured the time delay by the abrupt increase of neon flash Δt_{flash}.

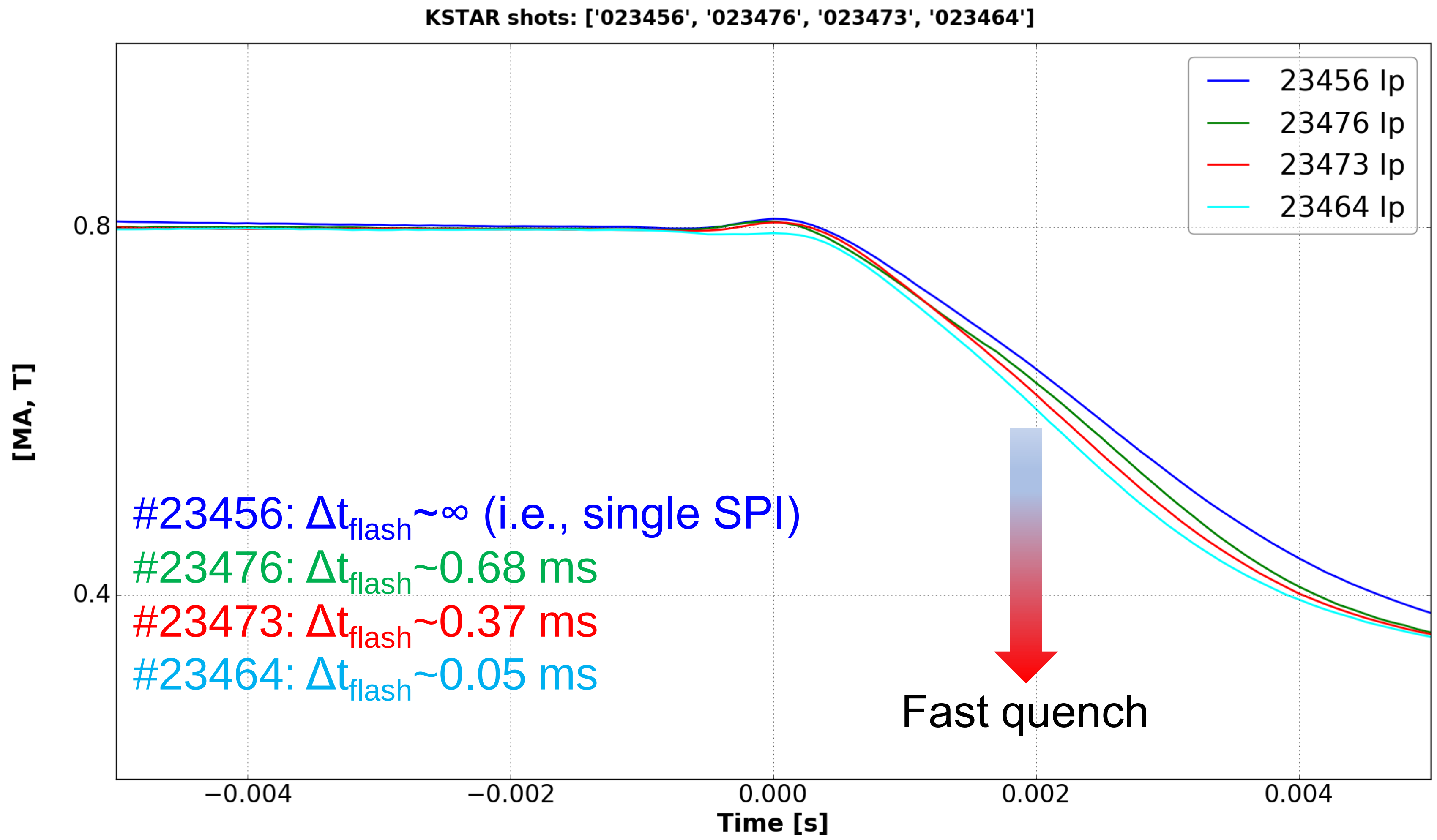

n=1 mode amplitude of exact synchronization was meaningfully low during thermal quench and the beyond in KSTAR

- How much does it affect the mixing of impurity?
- #23473 showed similar peak amplitude but rapid drop when compared to #23456 and #23476.

n=1 mode amplitude

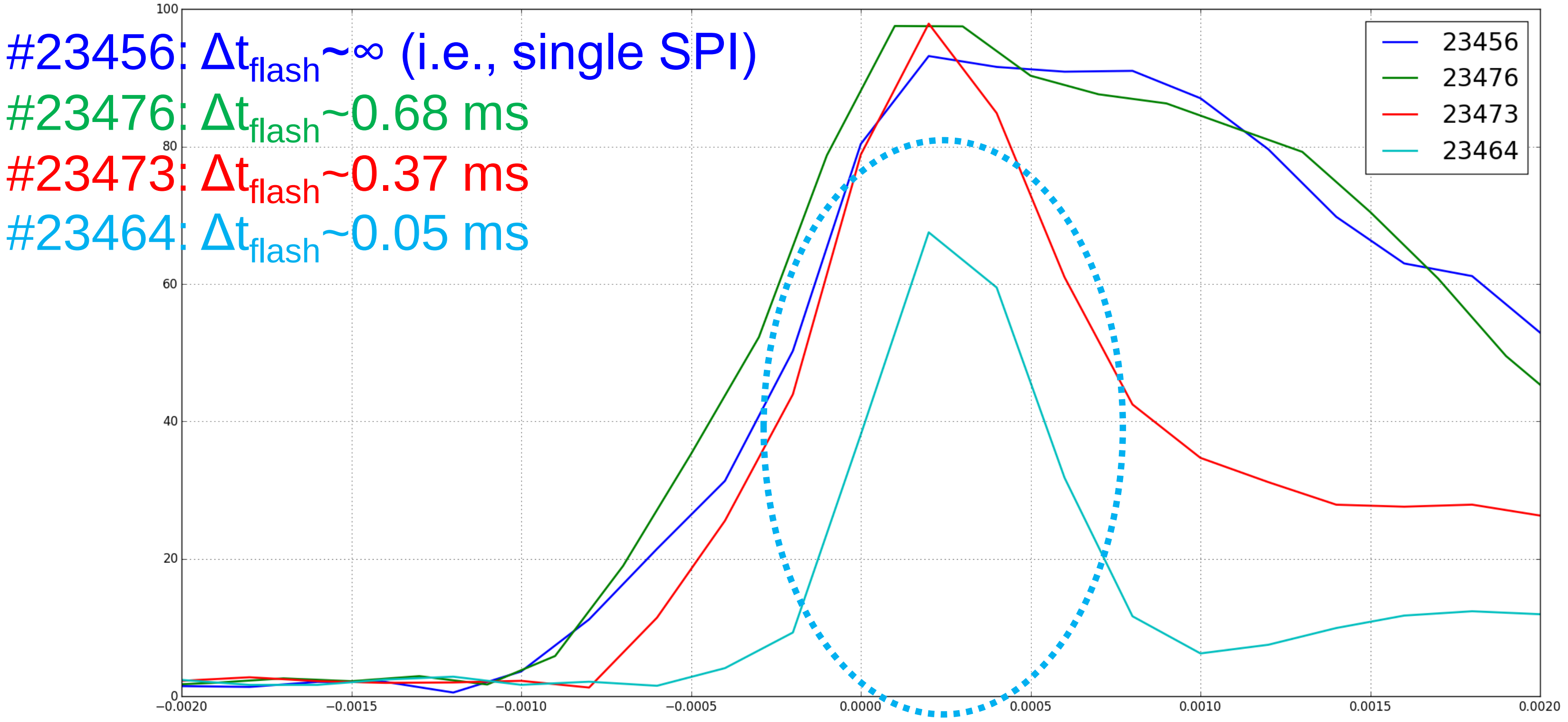

-0.002 Time to TQ end [s] +0.002

AUG Shattered Pellet Injector (SPI)

- ITER DMS TF project to install & operate an SPI
  - SPI provided by PELIN
- **Main goal: study the effect of SPI shard distributions**
- 3 separate barrels with different shatter angles 0, 12.5 and 25 deg
- H2, D2, Ne, Ar, D2+Ne pellets foreseen; D2 propelllant
- Lab commissioning & evaluation at IPP

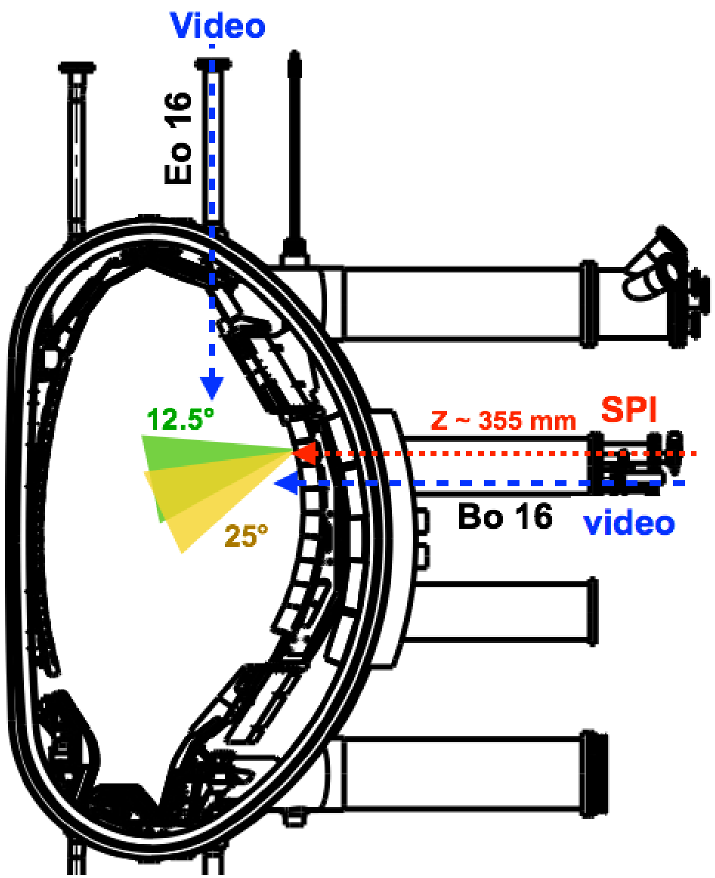

AUG Sector 16

SPI utilization – new diagnostics

- 3+1 fast cameras to provide 3-axis view of SPI shards and pellet integrity
- 5x new 4-channel foil bolometers
- 3 (V) + 1 (H) AXUV diode arrays, Σ 192 new channels

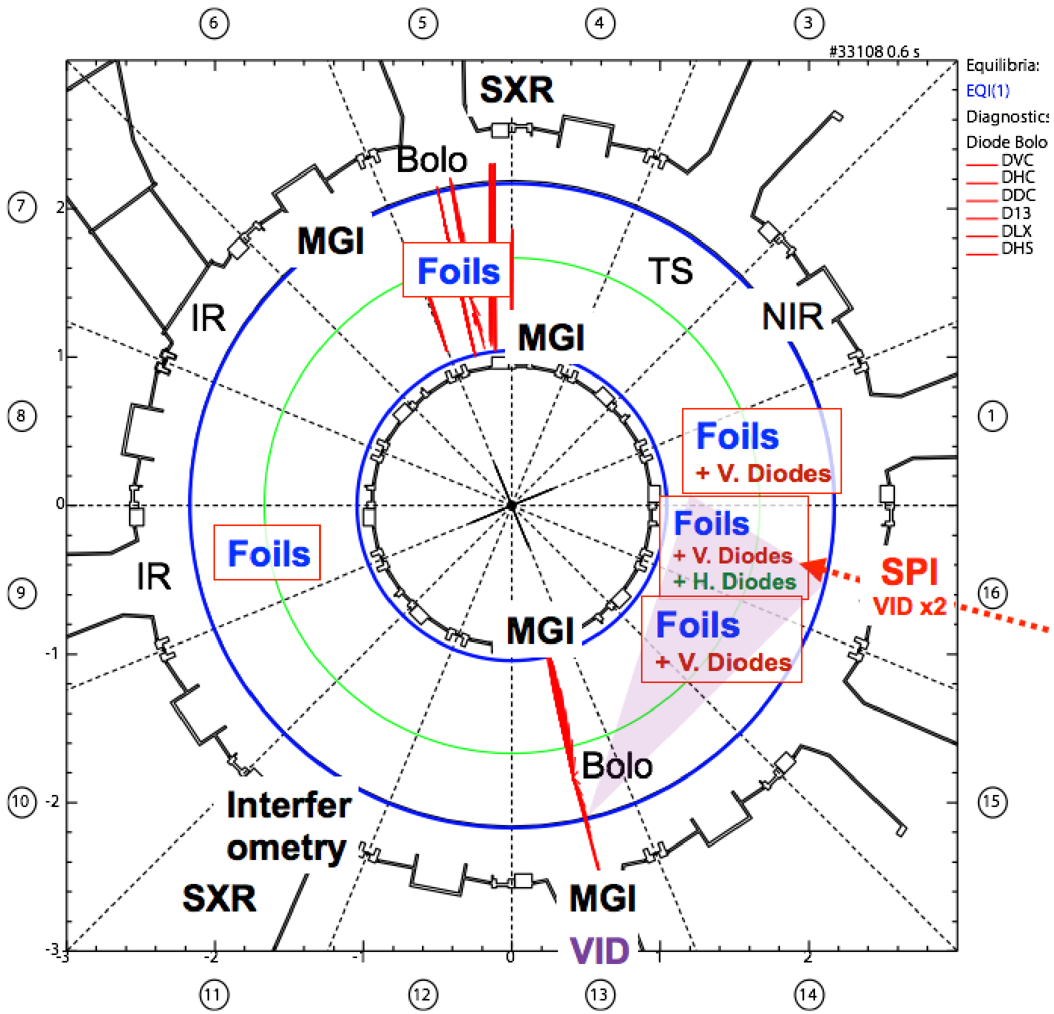

SPI schedule

- 2020 opening – AUG in-vessel work
  - – Bolometry, Bo16 shatter tubes, Eo16 video port
- 2021 early– SPI lab commissioning
- 2021 spring / summer – 1st AUG experiments
- (2021 opening – in-vessel modifications)
- 2022 – AUG SPI experiments 2nd round

Usual axisymmetric analyses give different outlooks regarding the ITER $f_{\mathrm{rad,th}} > 0.93$ requirement using SPI

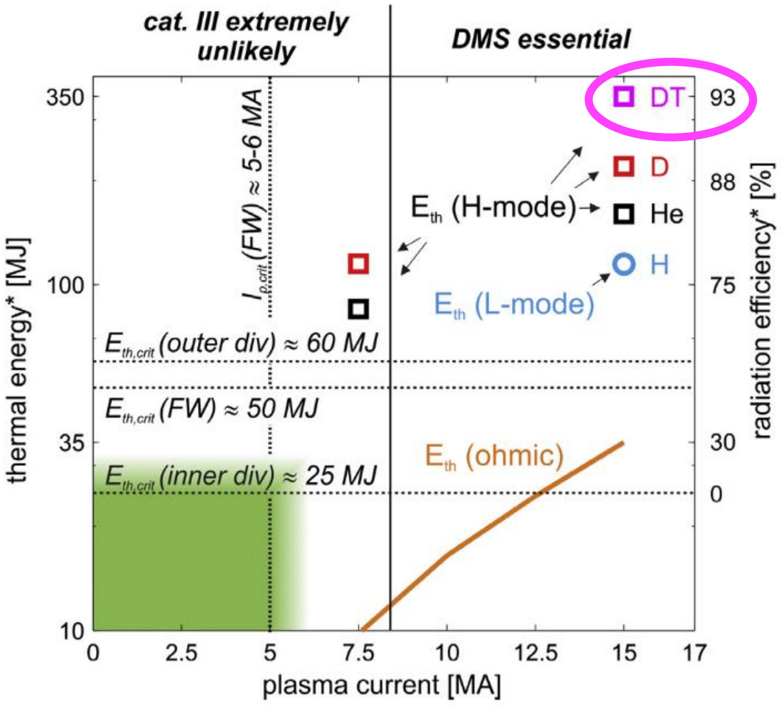

M. Lehnen et al., J. Nucl. Mater. **463** (2015) 39-48

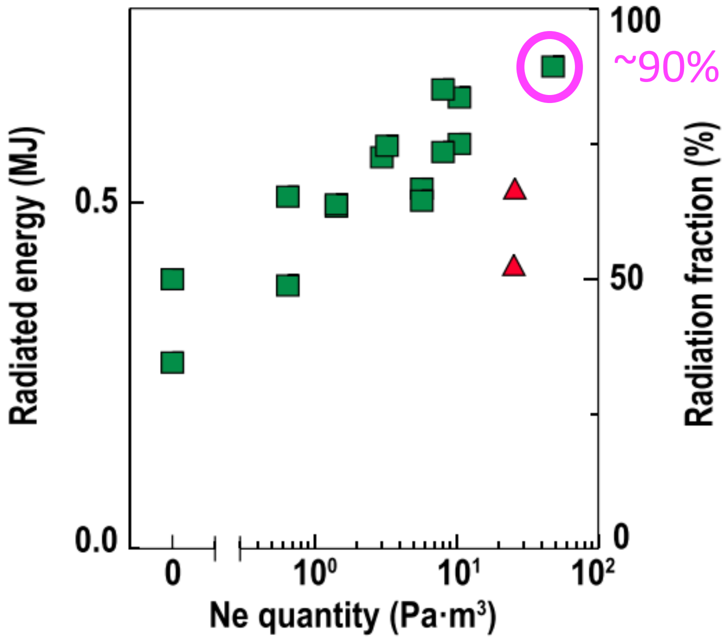

D. Shiraki et al., Phys. Plasmas **23** (2016) 062516

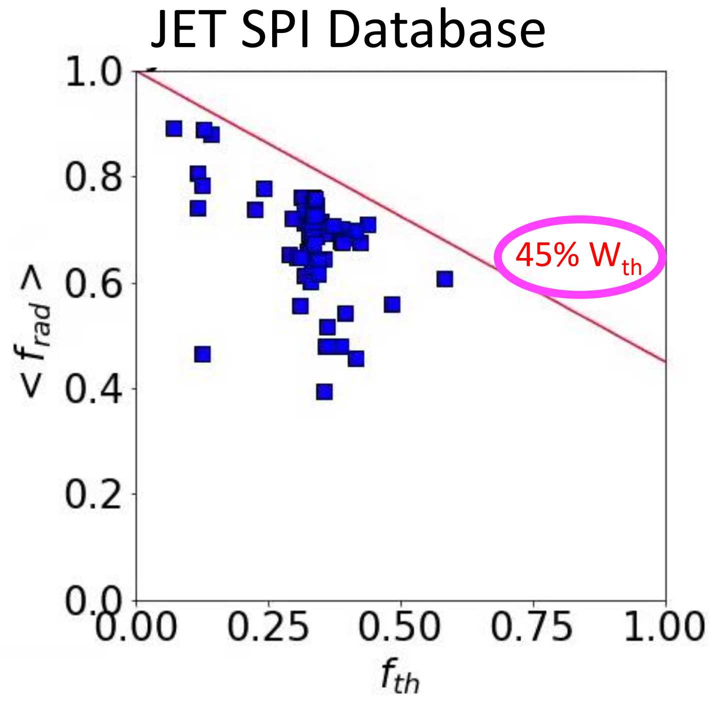

DIII-D NATIONAL FUSION FACILITY SAN DIEGO

EUROfusion

Conclusion: axisymmetric analysis is not sufficient for predictions of $f_{\mathrm{rad,th}}$ with error bars of order a few percent

Many independent DIII-D and JET studies find helical structures following SPI, providing the framework for 3D emissivity reconstructions

DIII-D NATIONAL FUSION FACILITY SAN DIEGO

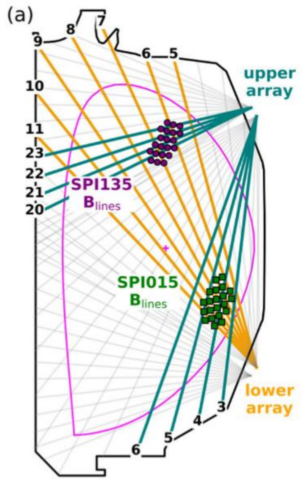

J. Herfindal et al., NF **59** (2019) 106034

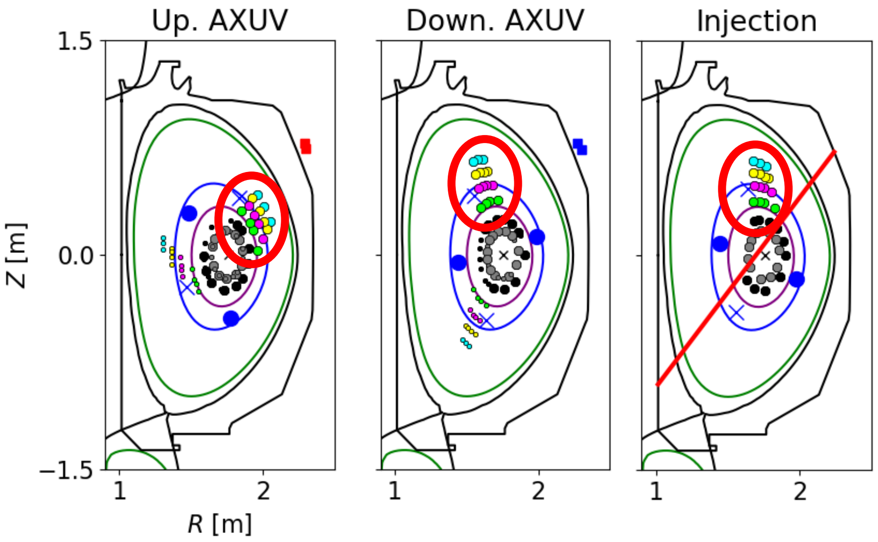

R. Sweeney et al., NF 2020, manuscript in review

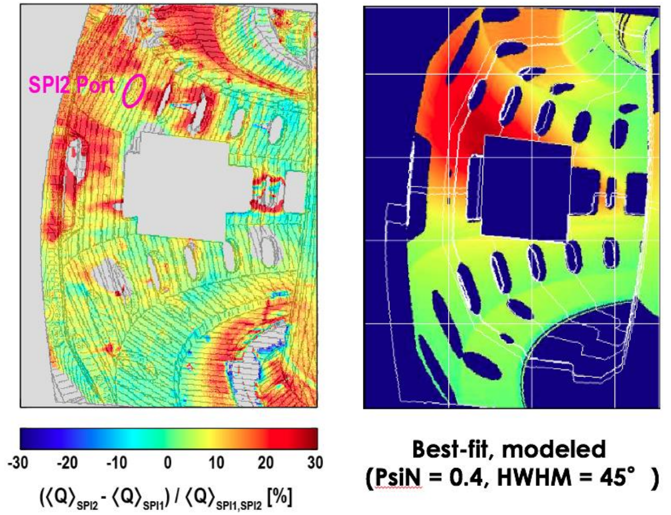

D. Shiraki, Disruption TF Meeting, June 25, 2020

Ohmic plasmas: error field seeded n=1

EUROfusion

Magnetic control of asymmetry

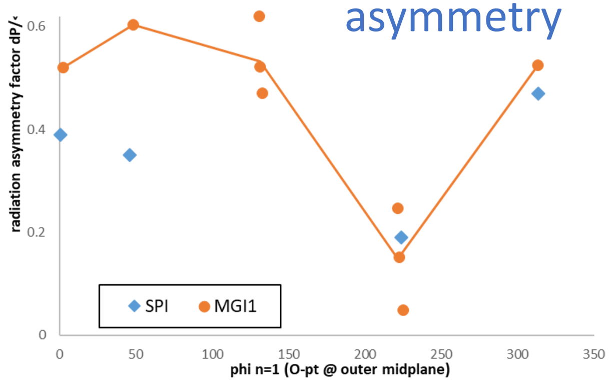

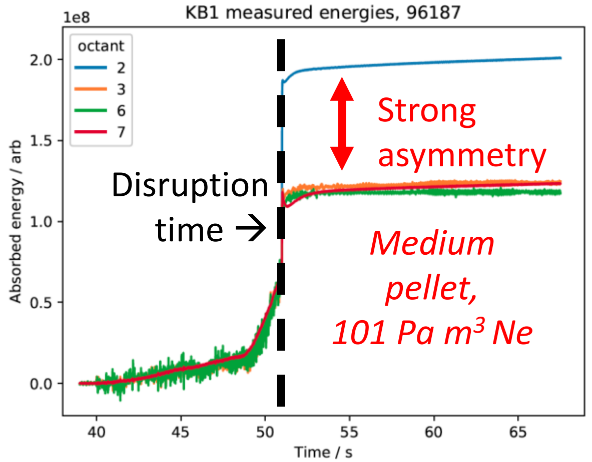

J. Lovell et al., RSI 2020, manuscript in review

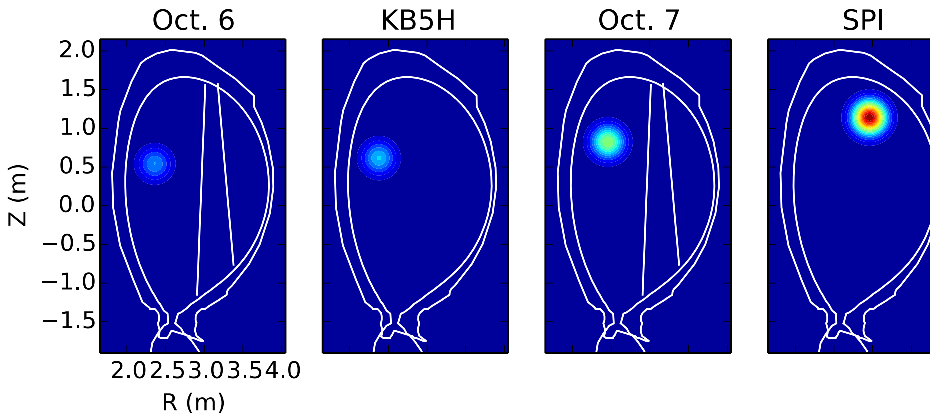

R. Sweeney et al., Phys. Plasmas 2021, manuscript in preparation

3D analyses of single SPI are finding toroidal peaking factors approaching 2, and preliminary radiated fractions of $f_{rad,th}$~0.45

Conclusions:

1. Peaking factors following **single SPI** may exceed ITER limit
2. Radiated fractions following **single SPI** may not reach 93%
3. Initial study of **dual SPI** on DIII-D exhibited degradation of the axisymmetric $\langle f_{rad,th} \rangle$
   [J. Herfindal et al., NF **59** (2019) 106034]
4. Further 3D studies (including KSTAR and J-TEXT) of single and many SPIs necessary to validate the ITER DMS requirements

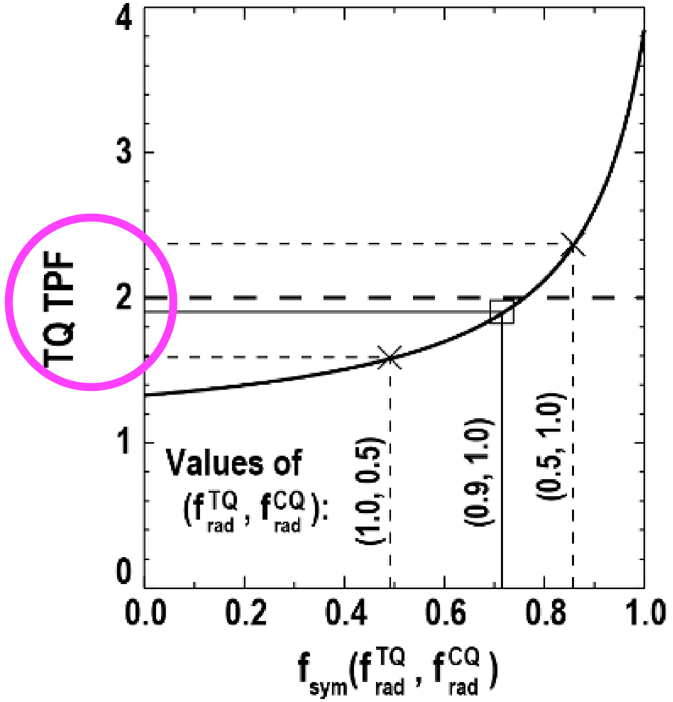

D. Shiraki, Disruption TF Meeting, June 25, 2020

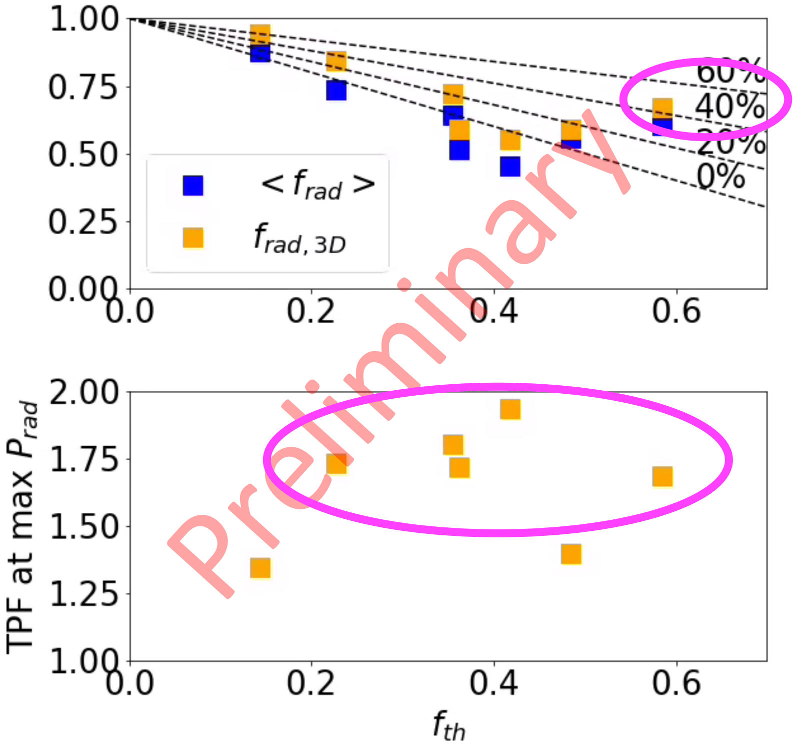

R. Sweeney et al., Phys. Plasmas 2021, manuscript in prep.

Conclusion

- ITER requires $f_{rad,th}>0.93$ and $PF<2$
- In DIII-D, axisymmetric thermal fraction $\langle f_{rad,th} \rangle$ approaches 0.9
- Decreasing $\langle f_{rad} \rangle$ observed with increasing f_{th} in JET
- Helical radiation is observed in DIII-D:
  1. Varying injection location changes radiation
  2. Toroidally separated AXUVs consistent with field-aligned structures
  3. IR analysis consistent with helical structure, and predicts $TPF=1.9{+0.5/-0.3}$
- Helical radiation is also observed in JET:
  - KB1 bolometers are consistent with a helical structure
- Constrained helical structure used in preliminary 3D radiated energy calculations; predicts $TPF\sim1.75$ and $f_{rad,th} \sim 0.5$
  - Sensitivity study to follow
- Magnetic control of radiation asymmetry in DIII-D unsuccessful, and JET experiments are inconclusive (more data to come)
- DIII-D dual injection results suggest a reduced f_{rad}; reason under investigation

Summary & Outlook

- JOREK simulation of both mono- and dual-SPI into ITER L-mode plasmas have been carried out with the two temperature model.
- The MHD destabilization mechanism is in accordance with previous understanding. **The MHD behavior correlates with the injection configuration in terms of symmetry. (Fig 1)**
- Short time difference between injectors cause remarkable changes in the dominant MHD response.
- **The toroidal radiation peaking factors remain mitigated even with asymmetry dual-SPI. (Fig 2)**
- D2 SPI simulation found possibility of strongly dilute the plasma before incurring the TQ, providing a scheme for suppression of hot-tail generation **(Fig 3)**

Summary & Outlook

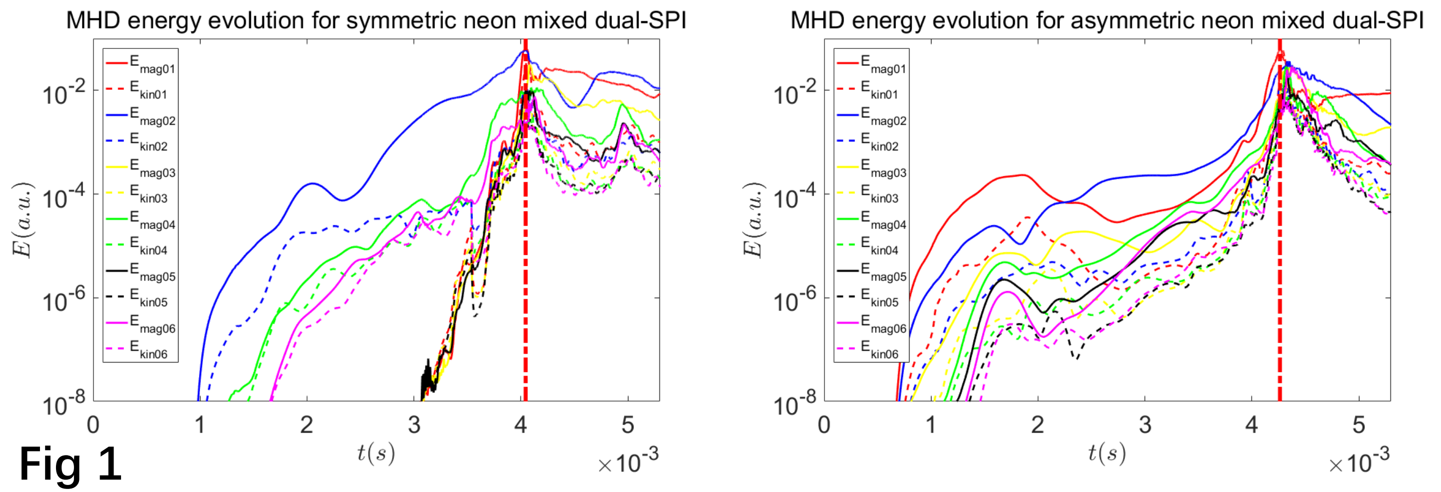

Fig 1

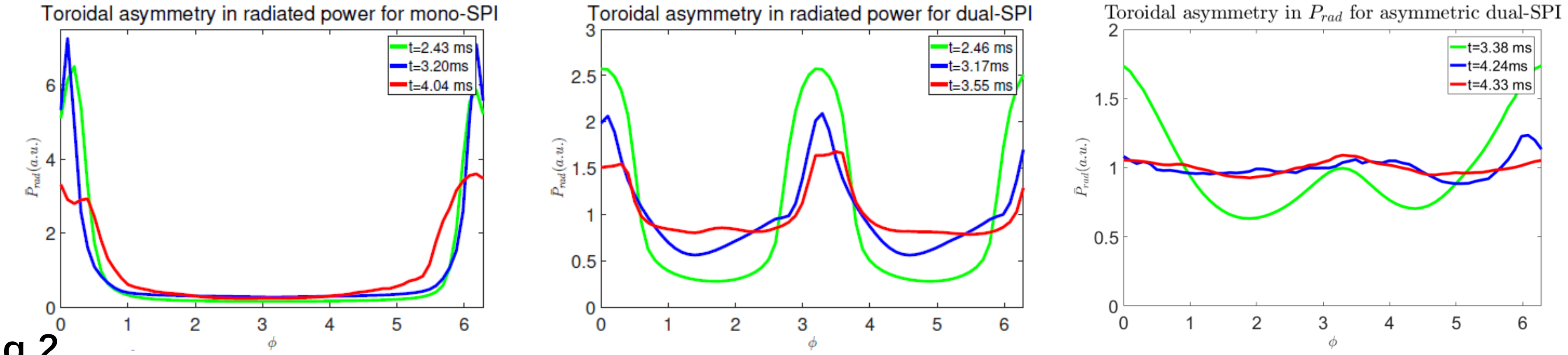

Fig 2

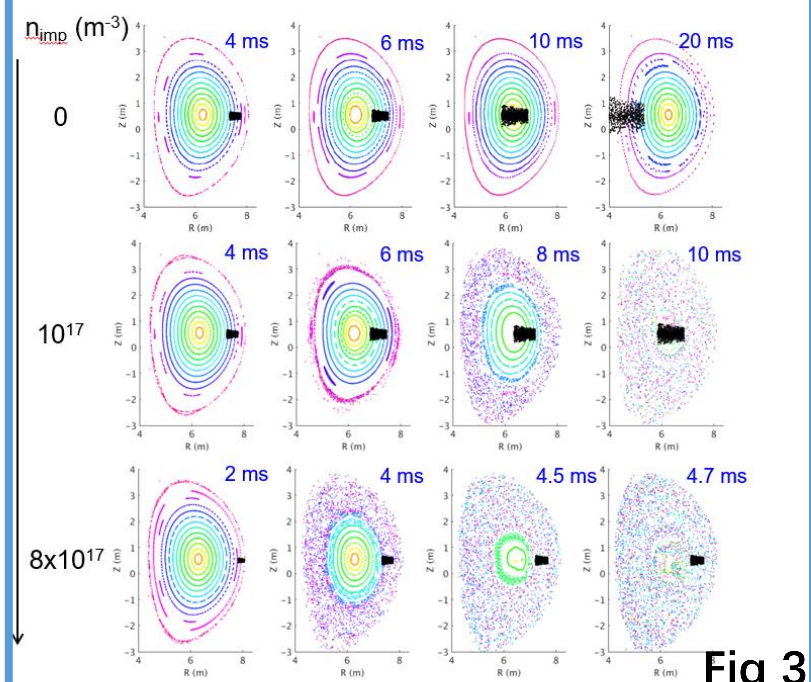

Fig 3

Summary & Outlook

- JOREK **non-equilibrium description** of impurity charge state distribution is underway. Continue to look into multiple injection scenarios. Working on treating the **hot-tail electron contribution** to the ablation rate properly as well as a **non-local ablation law**.
- M3D-C1 provides opportunity **to truly resolve the ablation cloud toroidally**, as well as **realistic wall coupling** and **accurate description of the impurity radiation**. Future development of **self-consistent runaway modelling** is promising. Will explore a variety of configurations.
- NIMROD has conducted preliminary **ITER H-mode pure neon simulation** with **non-equilibrium** impurity charge state treatment after the D2 fraction validation, and more high fidelity ITER simulations are underway. **Broad spectrum MHD activity as well as strong kink motion** are found to play significant role in the quenching process (similar observation in JOREK).

Major Results of Lyons et al. “Verification and Validation of Extended-MHD Modeling of Disruption Mitigation "

- **Verification studies**
  - M3D-C1 & NIMROD show quantitative agreement in 2D, nonlinear benchmark, JOREK differences likely due to its impurity model
  - M3D-C1 & NIMROD 3D nonlinear benchmarks
    - Axisymmetric, core deposition shows stable thermal quench, instability-induced current quench with large current spike
    - Injected, ablating pellet benchmark is underway
  - NIMROD viscosity & deposition scans show thermal-quench has expected dependence
- **Validation studies**
  - Initial M3D-C1 pellet-composition study shows qualitative agreement with DIII-D data, NIMROD shows quantitative agreement with experiment
  - M3D-C1 and NIMROD have begun modeling of recent JET & KSTAR experiments
  - JOREK shattered-pellet-injection modeling shows MHD-driven thermal quench

Lyons et al.: Verification Overview

M3D-C1/NIMROD MHD-impurity model benchmarked in 2D; JOREK shows discrepancy due to its impurity model

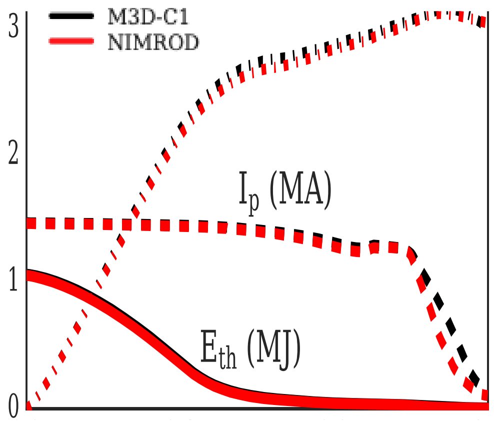

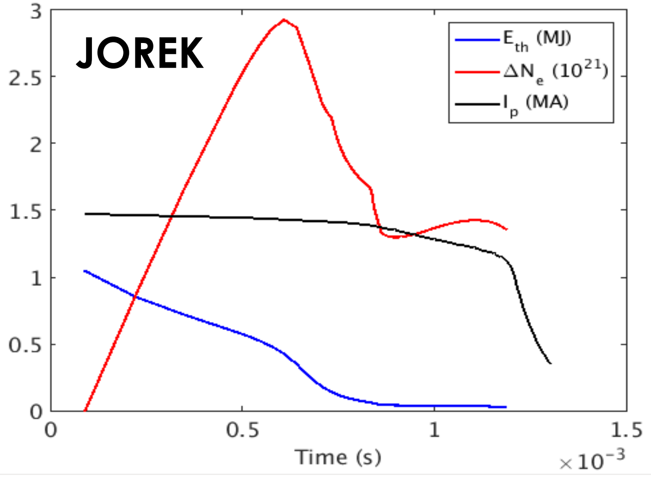

M3D-C1/NIMROD 3D benchmarks

Axisym. core deposition shows instability-induced CQ w/ Ip spike

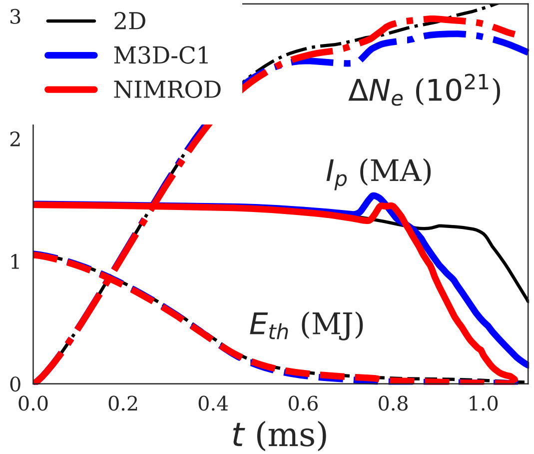

Pellet injection benchmark underway

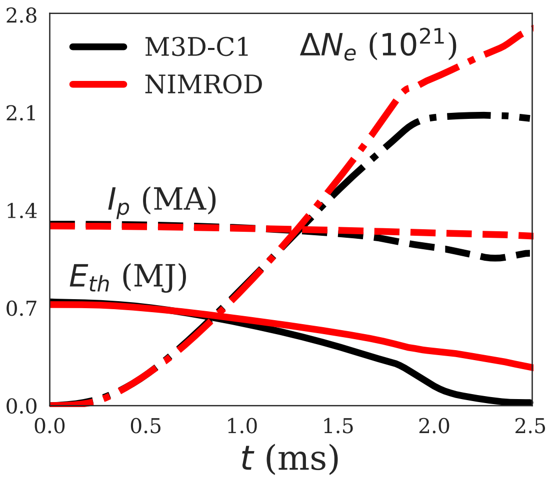

NIMROD parameter scans

Lower viscosity -> Shorter TQ & Less radiation

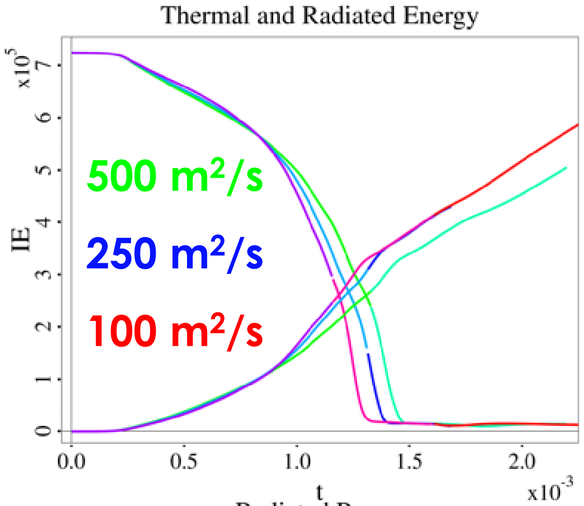

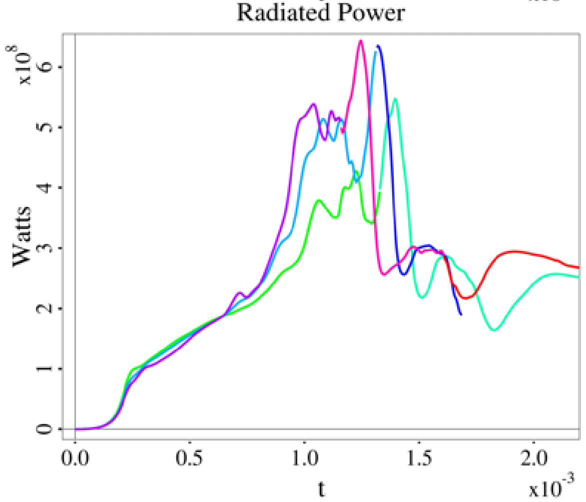

Lyons et al.: Validation Overview

Pellet composition on DIII-D

Initial M3D-C1 – Qualitative

Mature NIMROD - Quantitative

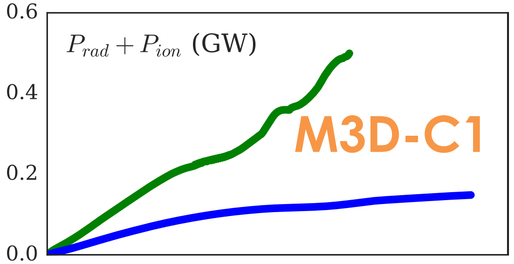

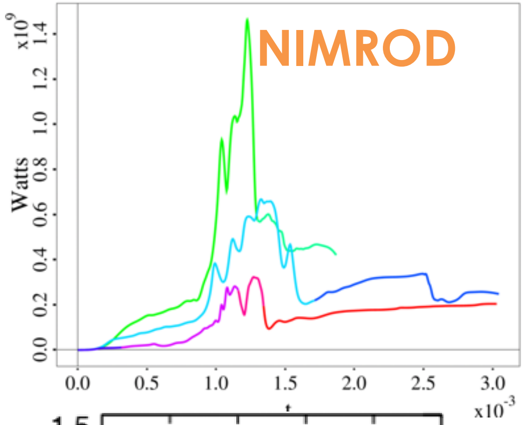

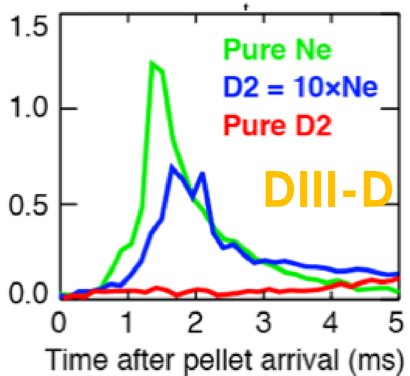

Initial M3D-C1 & NIMROD JET modeling: radiation-driven TQ

KSTAR modeling to begin shortly

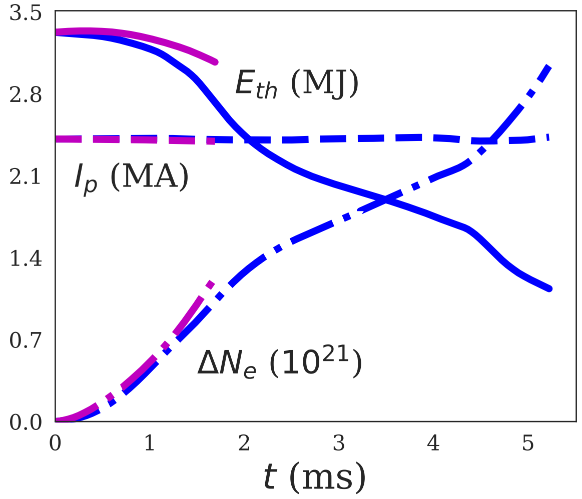

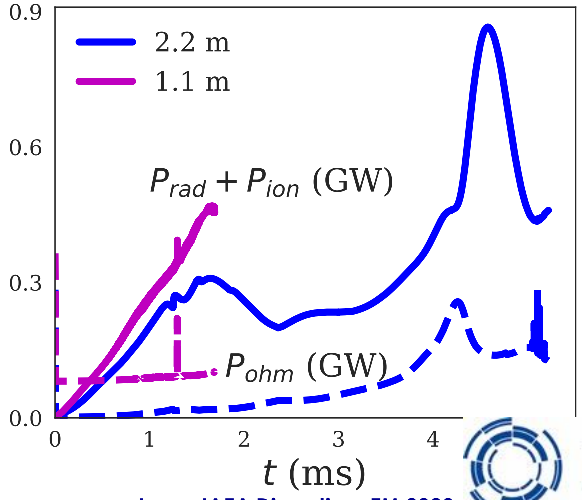

Lyons IAEA Disruptions TM 2020

EUROfusion

JOINT EUROPEAN TORUS (JET)

JOREK JET modeling

MHD activity (J_{phi} contraction & island formation) leads to complete stochasticization

Despite stochastization, core density low at late times

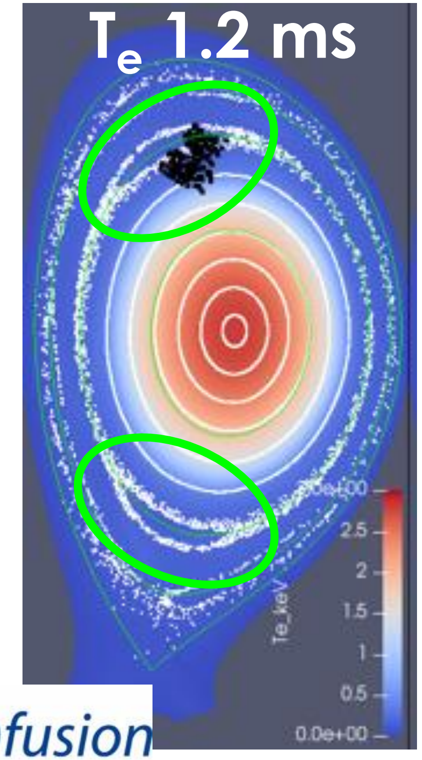

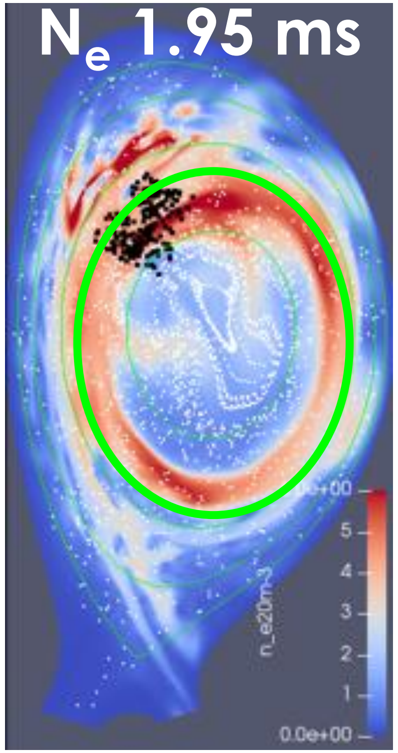

Injection schemes of SPI (especially for RE mitigation)

- D_2 injection and final kink loss of RE currents
  - 106. DIII-D Exploration of the D2+Kink Path to Runaway Electron Mitigation in Tokamaks
  - 132. Mitigation of runaway electron heat loads by deuterium SPI injection and kink activity
  - 136. Non-linear simulation of benign RE beam termination in JET D2 second-injection experiment

- Pure dilution cooling during pre-TQ and continuous/repeated SPI during post-TQ
  - 131. On the possible injection schemes with the ITER SPI system

Low Safety Factor (q_a) RE Beam Disruption Accessed in DIII-D Revealing Unique MHD Dynamics in Final Loss

- **Applied loop voltage (solenoid push) causes increased RE current in this shot**
- **Eventually reach q_a = 2**
- **Magnetic bursts get progressively larger as q_a = 2 is reached**
  - 1 kG kink mode → **$\delta B/B$ ~ 5%**
- **RE beam is promptly terminated by huge $\delta B/B$ (second disruption)**

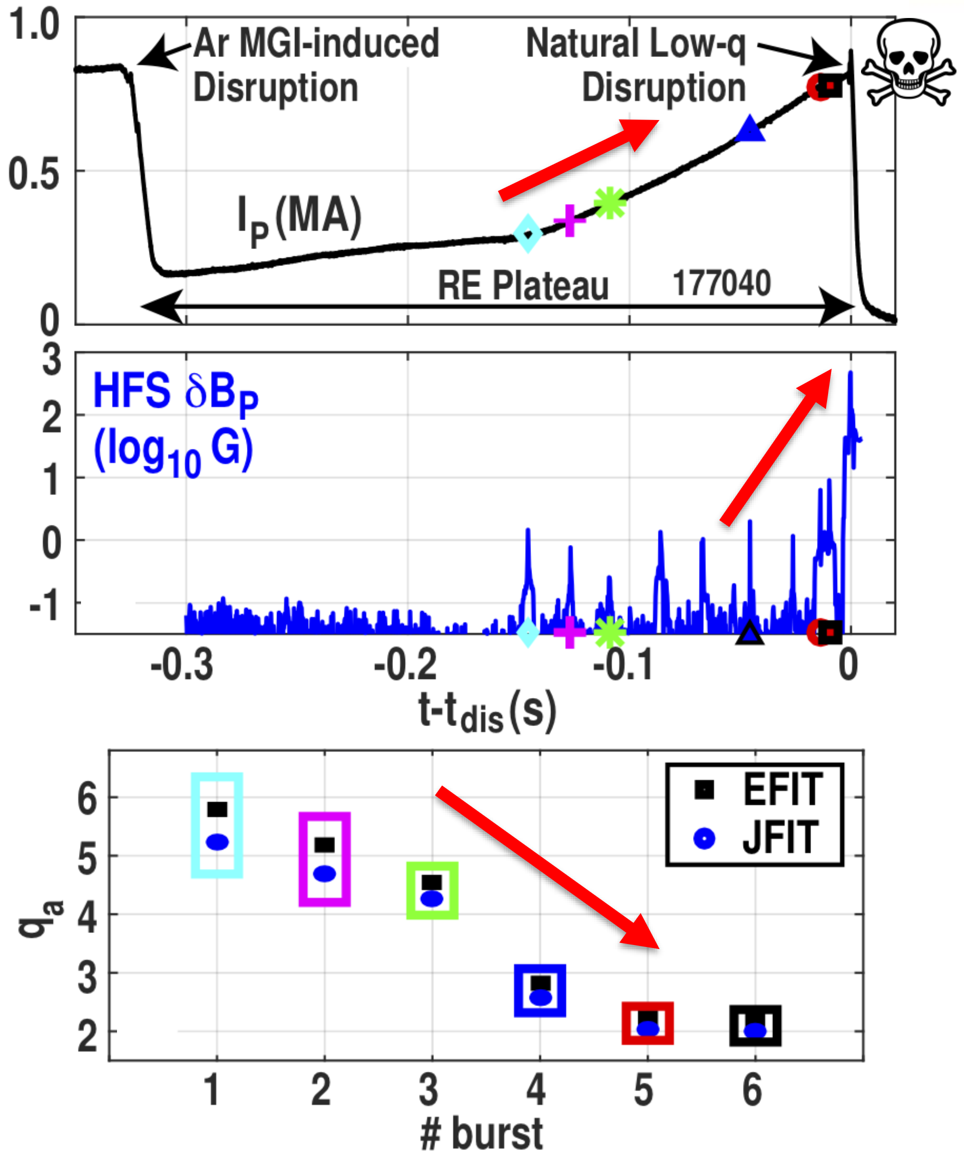

C. Paz-Soldan et al, PPCF 61 054001 (2019)

DIII-D NATIONAL FUSION FACILITY

Phenomenon seen with rising I_P, constant I_P & VDE. Can Access Low q_a Instability via Cross Section Contraction

Low Safety factor (q_a~2) achieved at constant I_P by

- Imposed cross-section shrinkage (outer PF push)
- Natural cross section shrinking during VDE

Requires High D_2 Purity to See Effect

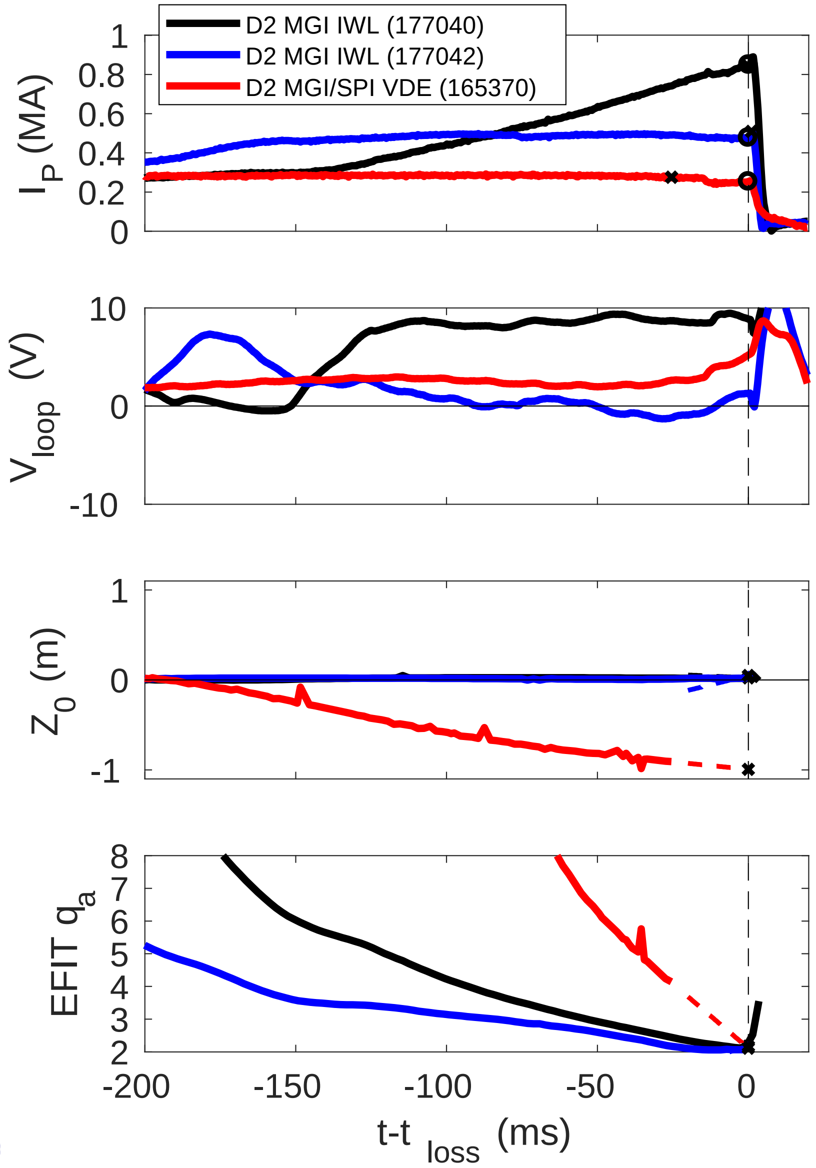

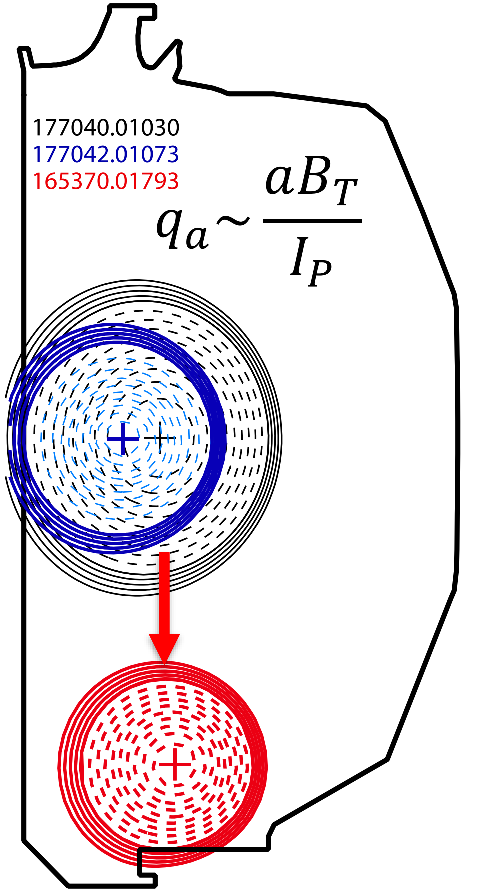

NATIONAL FUSION FACILITY

C. Paz-Soldc

Unpublished

Discharges with Same Program Can Fail to Reach q_a=2 D_2 Purity Was "Insufficient", But Mechanism Unclear

- **Same I_P & Shape Program**
  - Qty of Ar used to form RE differs
  - "Clean" vs "Dirty" Beams
- **Divergence of trajectories occurs when crossing q_a=3**
- **Dirty beams lose "D_2 purged state" and have minor current drops**
  - δB at q_a=3 similar – kinetic effect??

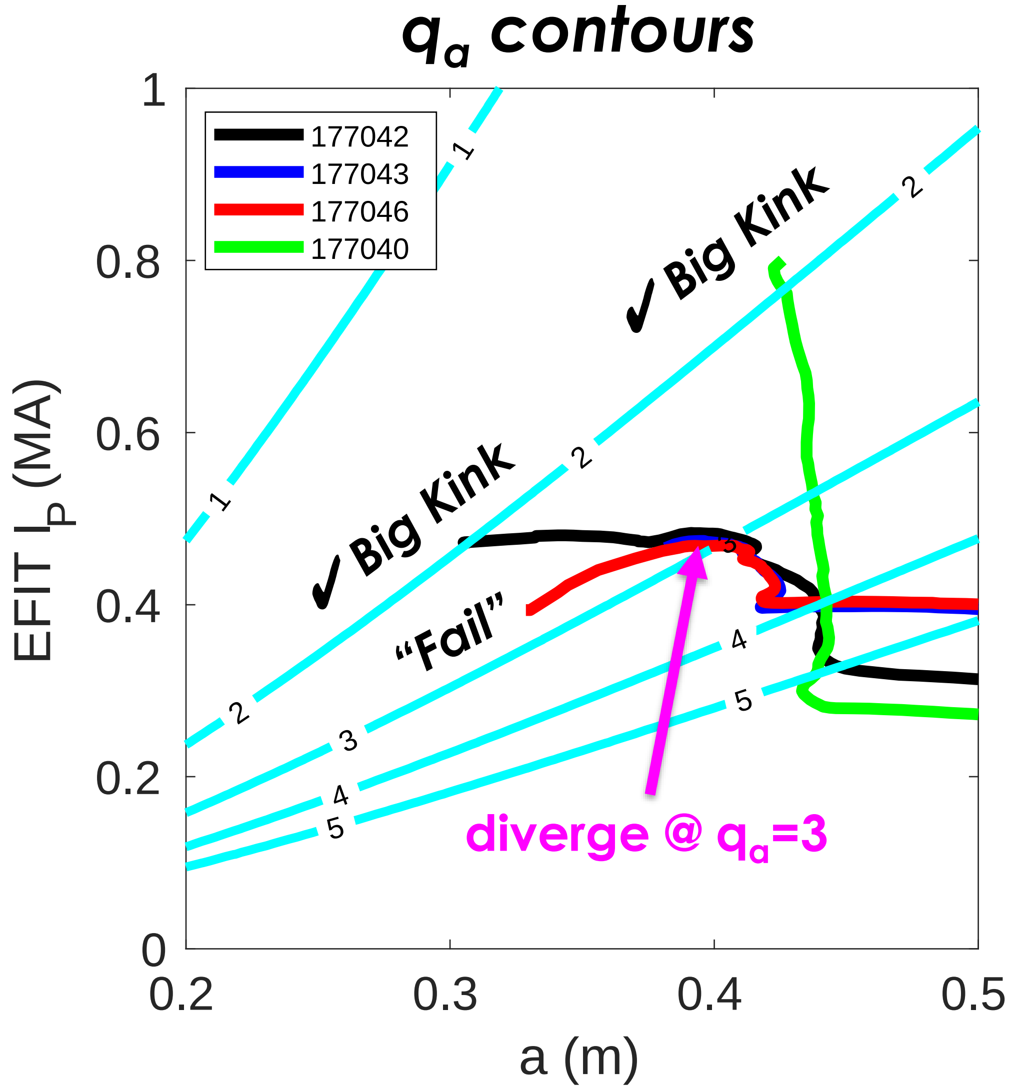

DIII-D NATIONAL FUSION FACILITY

Unpublished

D_2 SPI – JET and DIII-D

[Paz-Soldan PPCF 2019]

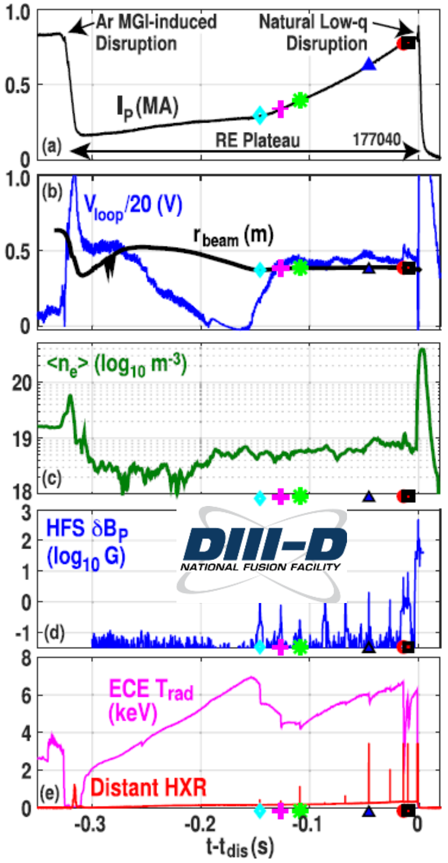

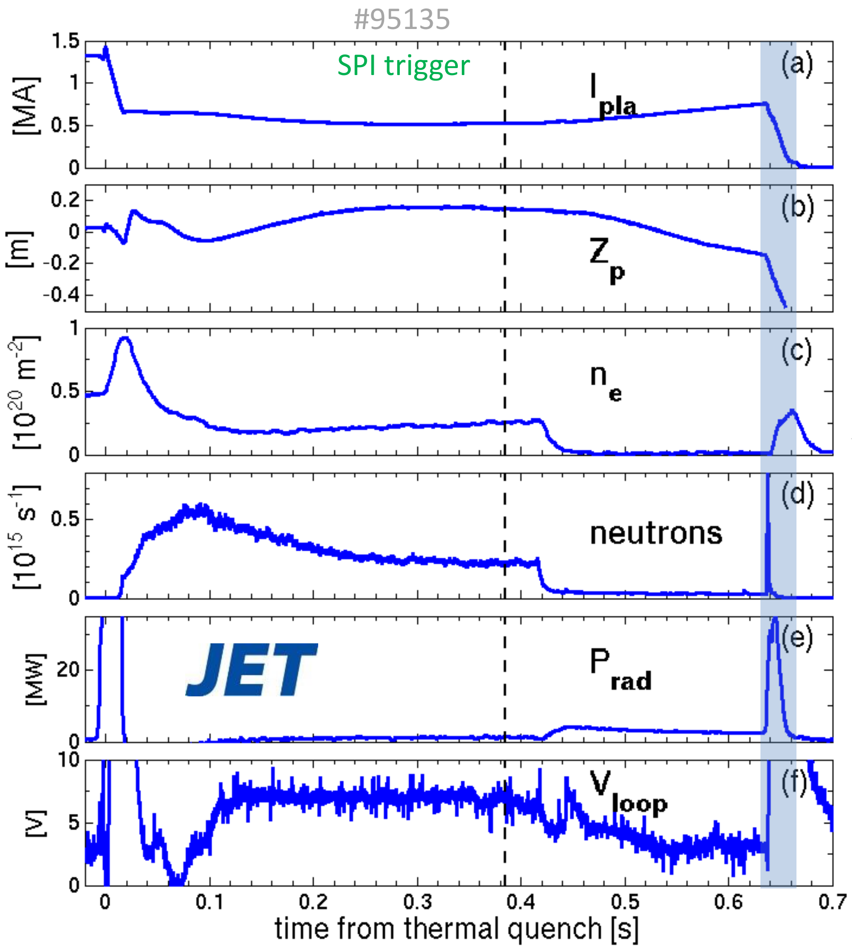

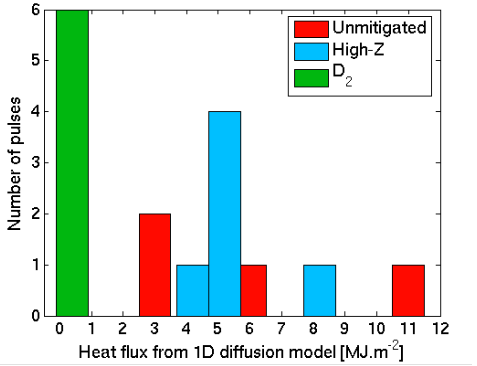

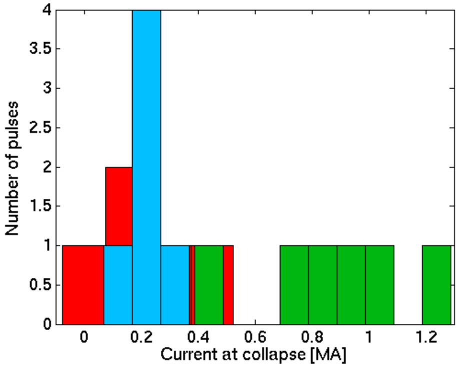

- D_2 mitigation of RE beams (SPI or MGI) lead to fast dissipation of REs on both JET and DIII-D
  - High-Z mitigation is not as efficient at JET
- D_2 purges the argon out of the companion plasma and leads to a RE current increase
- Up to 1.27 MA of runaways dissipated without impacts on the wall
- Key elements: large instability and absence of RE re-acceleration during the final collapse

Role of the MHD instability

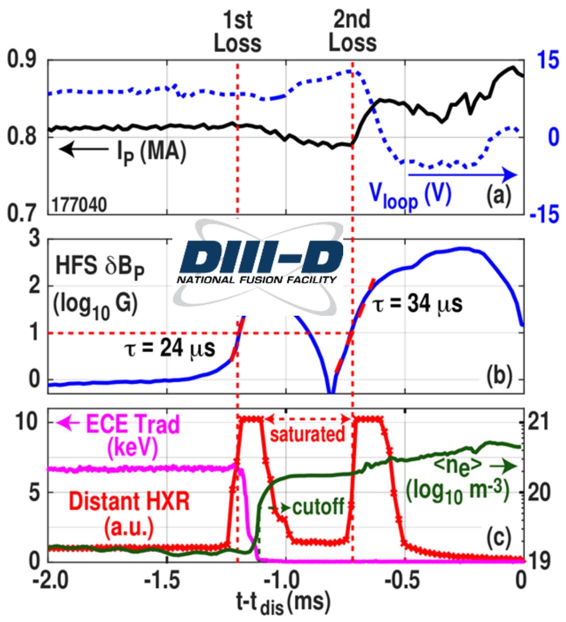

[Paz-Soldan, PPCF2019]

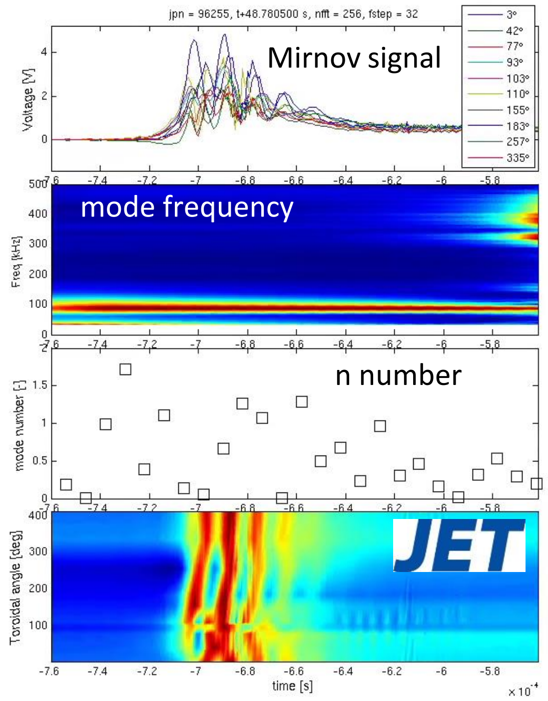

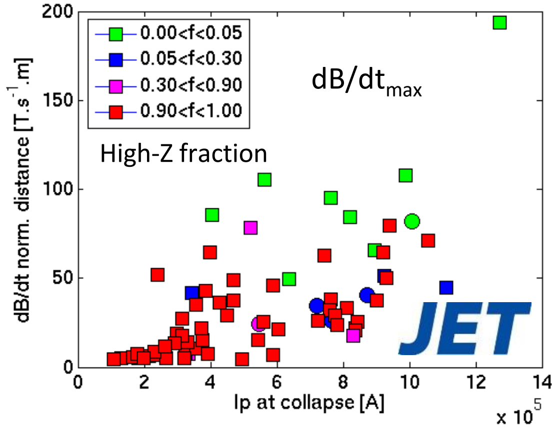

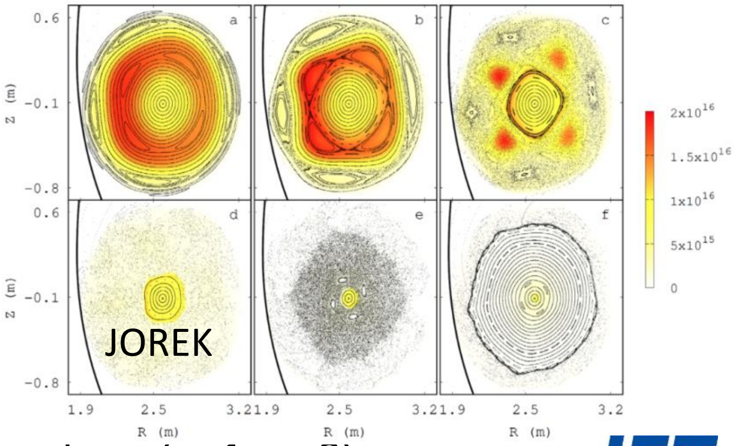

- Instability develops on 10-50 μs timescale, mostly low n numbers (n=1, n=2)
- No precursor, but some pre-existing islands (JET) or intermedaite crashes (DIII-D)
- All benign cases have short MHD growth rates (dB/dt) but some high-Z benign too
- Evidence of a hollow profile at JET, possibly linked to the pre-collapse current increase?
- MHD simulations (JOREK, MARS-F) confirm a consistent picture of a 50-100 μs instability deconfining >90% of runaways

Companion plasma purity – RE reacceleration

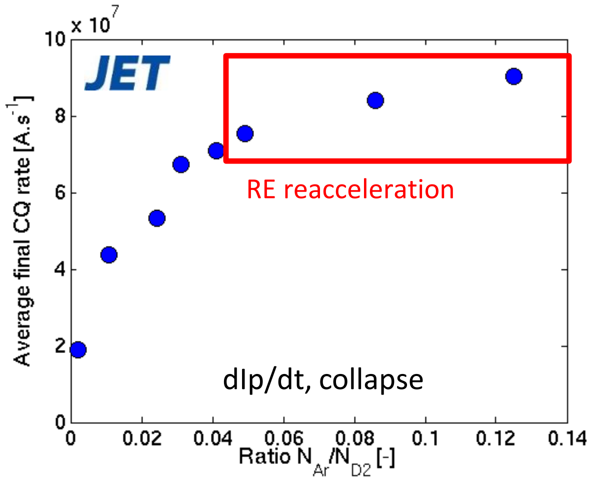

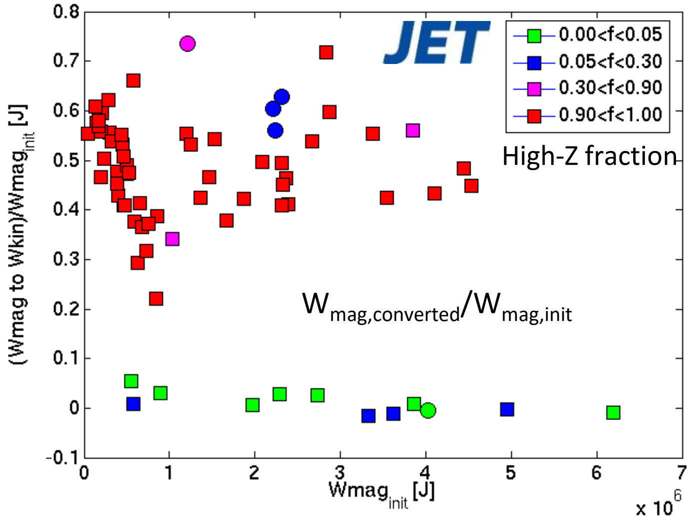

[Hollmann PoP 2020]

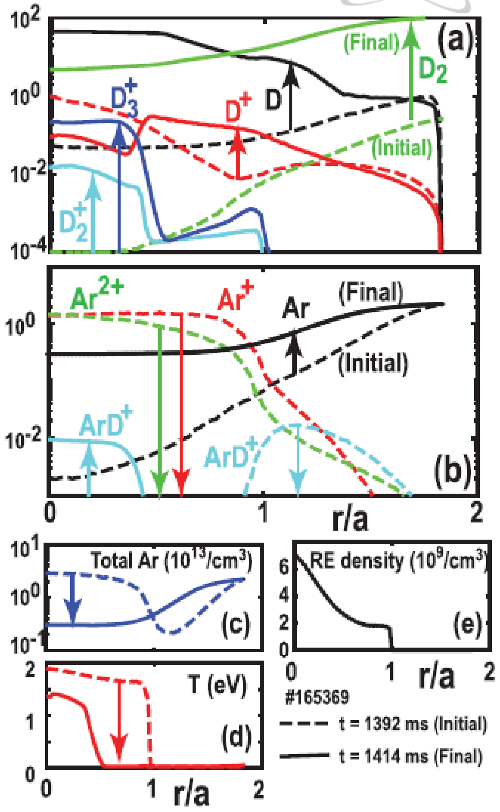

- D_2 « purge effect » confirmed by 1D diffusion simulations on DIII-D
- Purge incomplete at JET: enough remnant argon in the companion plasma cancels the D_2 effect
  - Signs of reacceleration of runaways above a certain argon fraction
  - Pure high-Z non-benign cases: probably continuous reacceleration
- Final collapse timescale and radiated power depend on the argon remnant
- An imperfectly purged companion plasma leads to conversion of RE magnetic energy into kinetic energy

RE beam mitigation by D_2 needs:
- A Large MHD instability
- A pure enough companion plasma

Bandaru et al., JOREK simulation of benign RE beam termination in JET

- JOREK simulation of fast MHD activity leading to benign RE loss in JET
- RE fluid model coupled to background plasma
- Hollow equilibrium profile before the crash

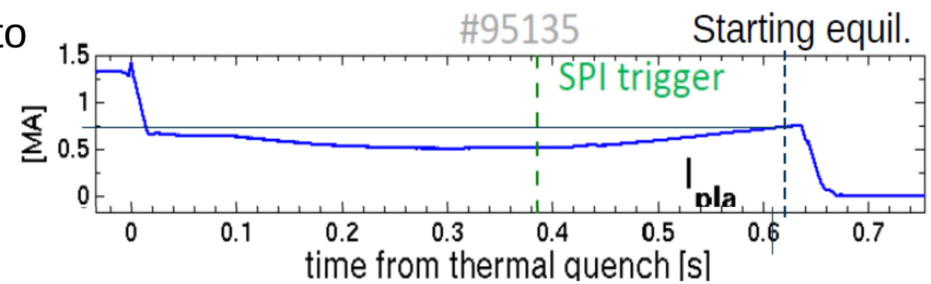

Equilibrium

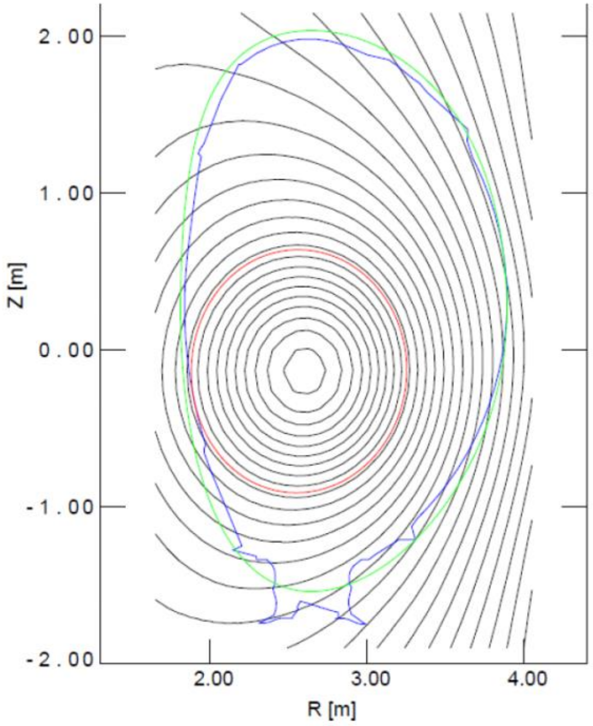

Poloidal magnetic energy

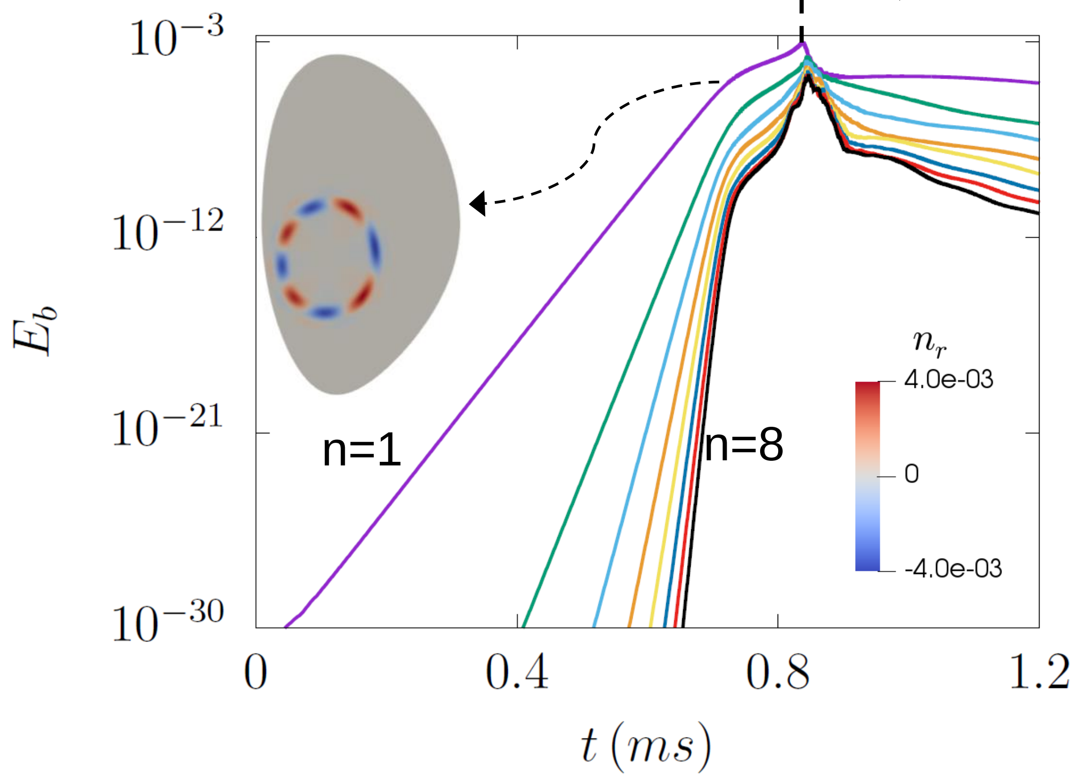

Bandaru et al., JOREK simulation of benign RE beam termination in JET

Stochastization leading to fast RE losses

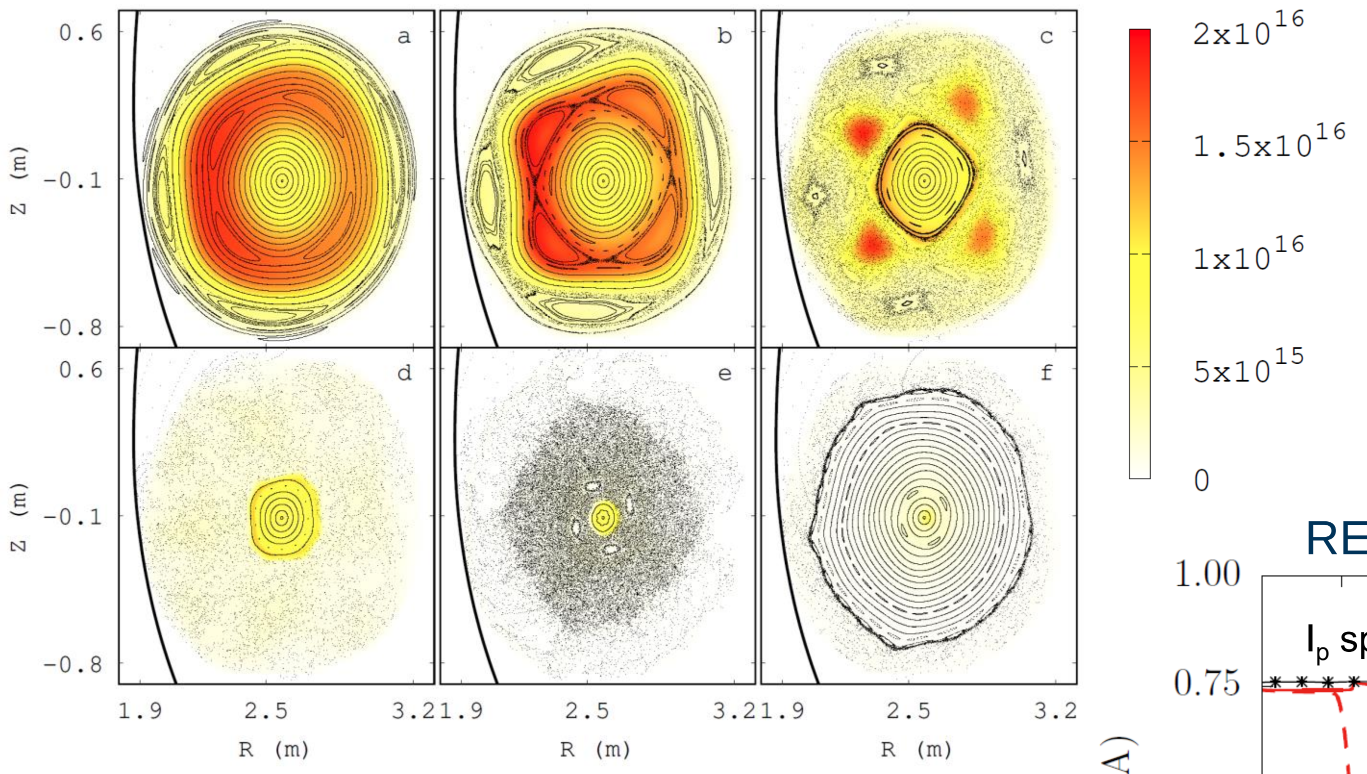

RE loss and current spike

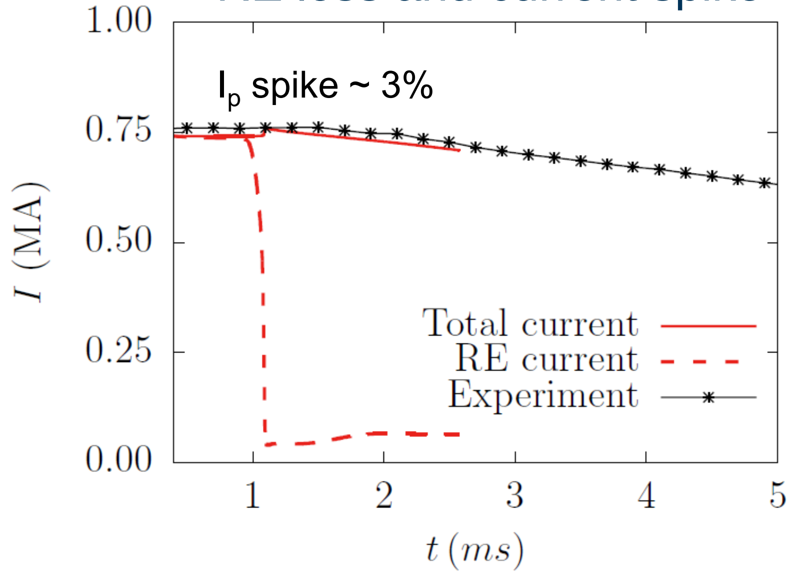

Excellent match of key MHD physics with experiment

Pre-TQ pure D_2/H_2 SPI…

…could be the best hope to raise n_e, which may be critical for RE avoidance [Martín-Solís, NF 2017], and in particular for hot tail generation avoidance thanks to pre-TQ dilution cooling

Key point: D_2/H_2 only produces a « lukewarm » front, leading to minor MHD destabilization

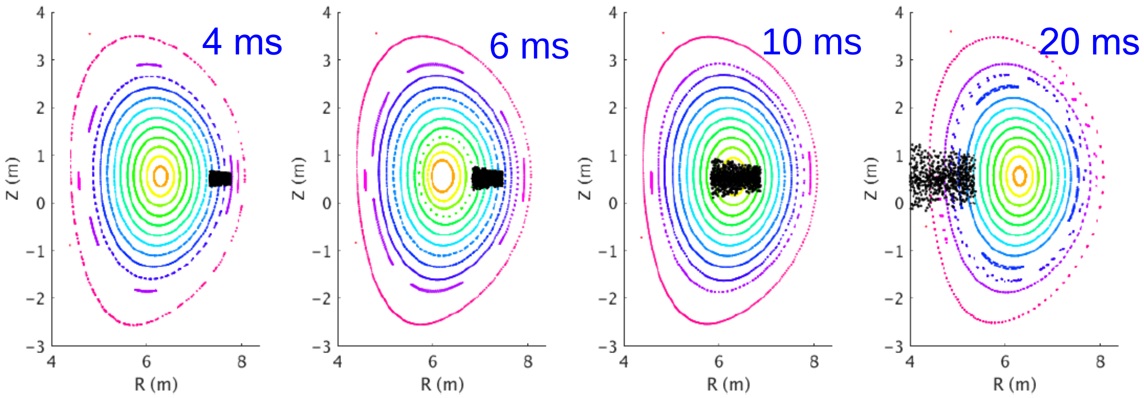

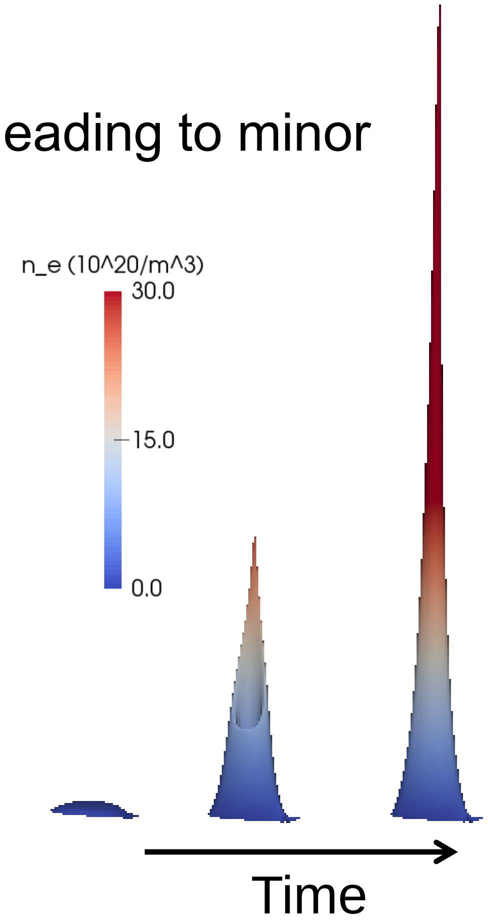

- Motivates detailed studies regarding:
  - Effect of background impurities
  - Effect of pre-existing islands
  - Compatibility with other DMS objectives

For more detail:
http://arxiv.org/abs/2006.16020

Repeated post-TQ (S)PI…

…might be able to deplete RE seeds before they avalanche too much

Key idea: exploit RE energy loss each time they travel across shards

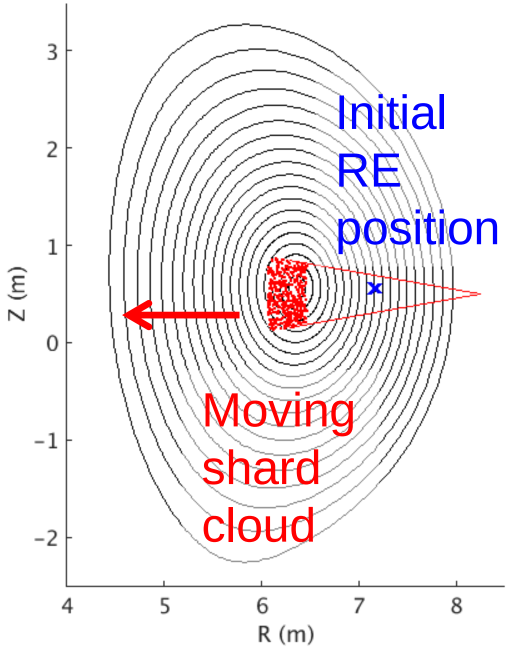

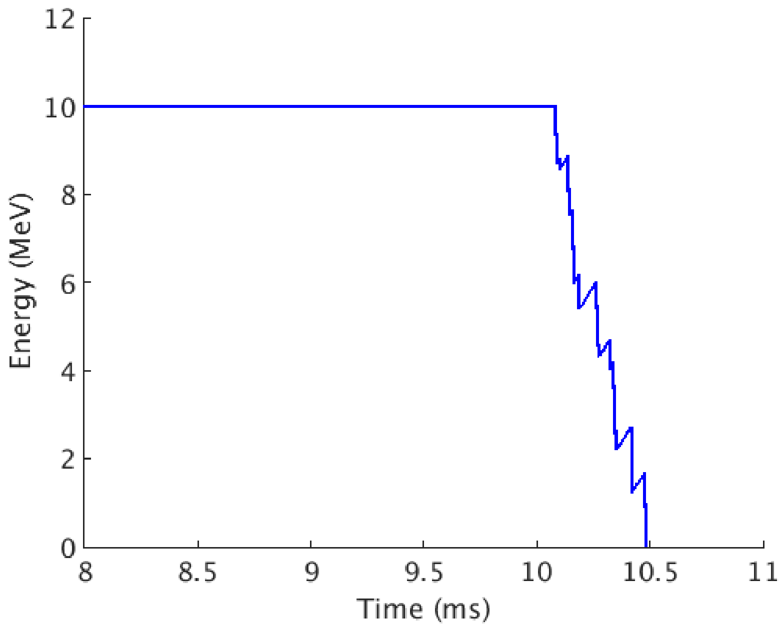

Required pellet number appears prohibitive for H_2, but might be within ITER DMS capabilities for Ne or Ar… However Ne or Ar are likely to make the CQ too short

A very interesting idea suggested by N. Eidietis: use shell pellets to combine large stopping power of high-Z pellet core with small effect on CQ duration from low-Z pellet coating

For more detail: http://arxiv.org/abs/2007.01567

Pellet/shards dynamics: shattering, ablation/sublimation, assimilation

- Shattering process: geometry of shattering tube and propellant gas effect
  - 127. Shatter Plume Analysis from the JET, KSTAR, and DIII-D Shattered Pellet Injectors

- Pellet ablation/sublimation
  - 151. Near-field models and simulation of the ablation of pellets and SPI fragments for plasma disruption mitigation in tokamaks
  - 148. Pellet sublimation and expansion under runaway electron flux

- Assimilation of pellets (with companion plasma)
  - 117. Particle Assimilation During Shattered Pellet Injection
  - 134. Study of the companion plasma during runaway electron mitigation experiments with massive material injection in the JET tokamak

Shatter Tube Designs

- Various shatter tube designs have been lab tested and implemented on tokamaks over the last ~12 years
- All designs are capable of shattering pellets and the fragment size distributions for single impact designs are mostly understood (angle and pellet speed dependent).

OAK RIDGE National Laboratory

Propellant gas issues

- The SPI test setup in the ORNL pellet lab did not have any effective pumping gaps to remove propellant gas
- This was thought to have a major impact on the dynamics of the shatter plume
- Pellets were fired without any major changes then modifications were made to remove an estimated 80% of the propellant gas, then a second round of shots was conducted

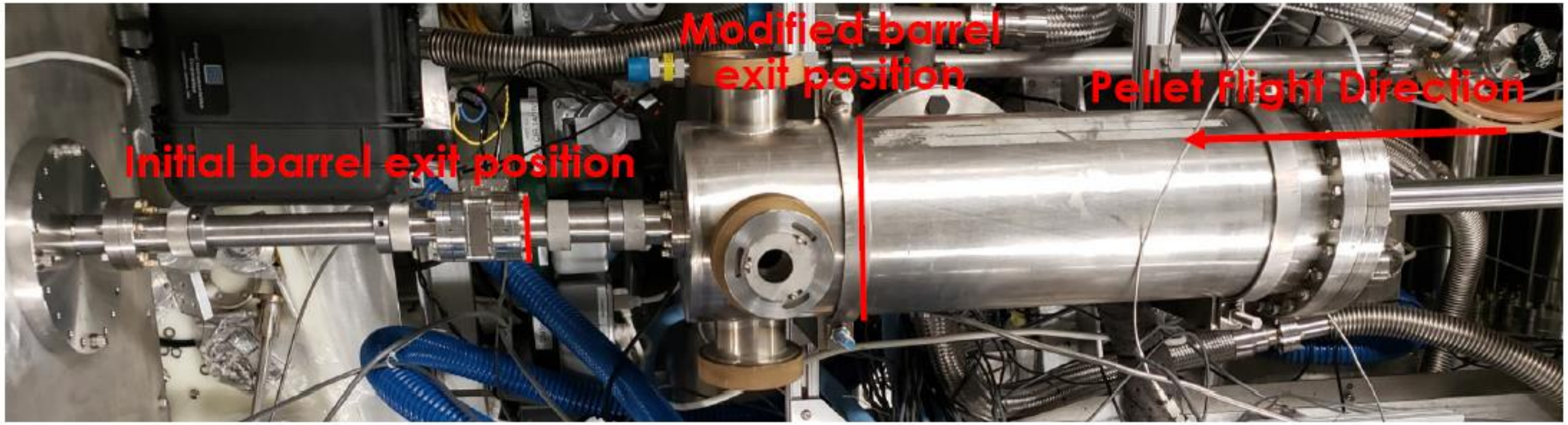

Oak Ridge National Laboratory
US iter

Conclusions/General Thoughts

- The modifications made to reduce propellant gas down stream resulted in a significant change in plume dynamics
  - Smaller particles at the rear of the plume stretch out over a longer time than without gas, previously accelerated by excess gas (hypothesis)

- No statistical difference in fragment size distribution between gas and reduced-gas cases, also no difference between 20-degree miter bend (similar to DIII-D and KSTAR) and JET shatter tube

- Fragments at the front of the plume are traveling significantly faster than the fragments at the end, resulting in a possible large spread over a long distance
  - Forces (or gas) generated during shattering process accelerates small fragments at front of plume and slows fragments at rear of plume (hypothesis)

- The bulk of the mass is located after a very small initial segment of plume, which consist of very small fast fragments

- The initial pellet speeds were not measured, but the speeds of the bulk of the plume seem to somewhat coincide with the assumed nominal speeds of these pellets

- The comparison of the JET ST with the 20-degree miter bend shows that with the propellant gas entrained, there is no significant difference in fragment size distribution, plume spread, or plume duration

Introduction: near-field models and codes for pellet ablation

Near-field Model

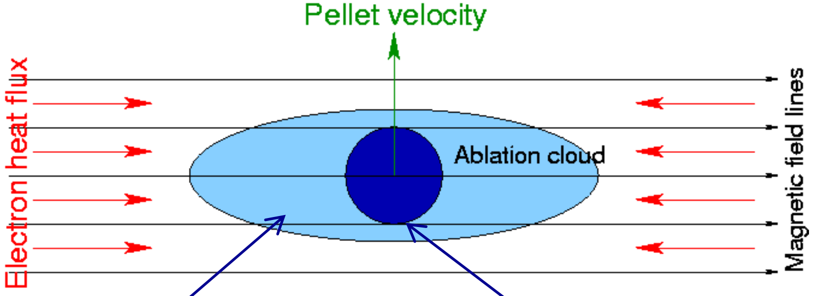

- Phase transition (ablation model) for pellet surface

- Kinetic model for the electron heating
- Low magnetic Re MHD equations
- EOS with atomic processes, radiation
- Grad B drift models for ablated material
- Pellet cloud charging models

Near-field Codes

FronTier (FT)

- Hybrid Lagrangian-Eulerian code with explicit interface tracking
- Both pellet surface and ablation cloud – plasma interface are explicitly tracked
- 2D axisymmetric simulation of the ablation of single neon or deuterium pellets, computing ablation rates
- Main role: V&V, verification of adaptive 3D Lagrangian particle code

FT simulation of neon pellet in 2T magnetic field

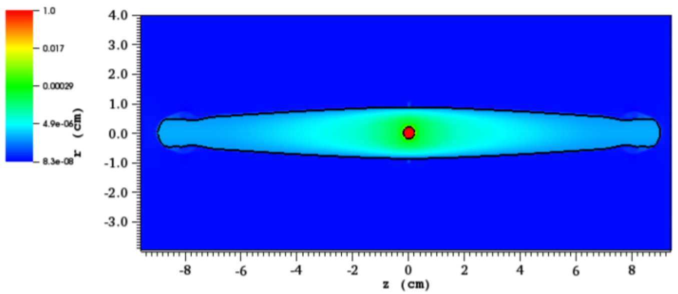

Lagrangian Particle code (LP)

- Highly adaptive 3D particle code, massively parallel
- Lagrangian treatment of ablation material eliminated numerous numerical difficulties associated with ambient plasma, fast time scales etc.
- Supports many SPI fragments in 3D
- R. Samulyak, X. Wang, H.-S. Chen, J. Comput. Phys., 362 (2018), 1-19.

LP simulation of neon pellet in 2T magnetic field with grad B drift (left) and SPI fragments (right)

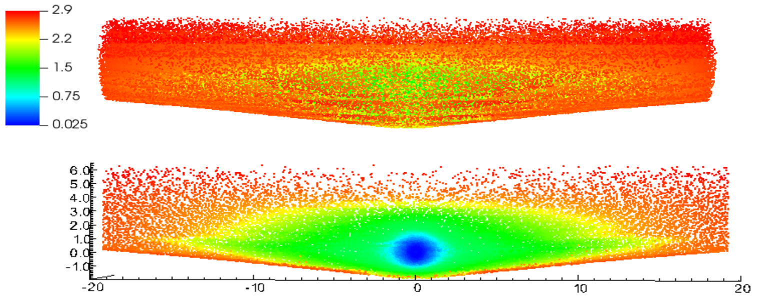

Reduction of the ablation rate in magnetic field for neon pellets: fixed shielding length compared to self-consistent shielding length

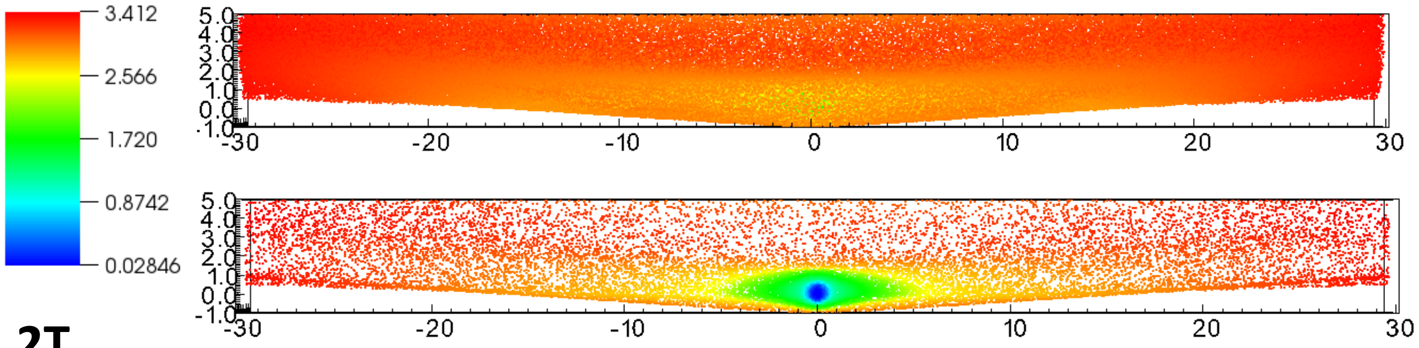

2T

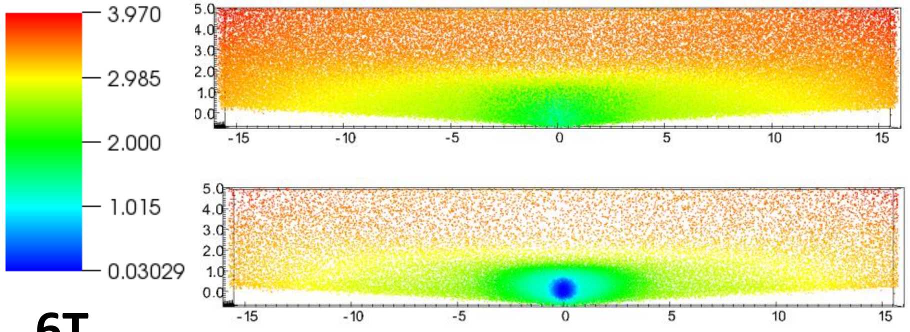

6T

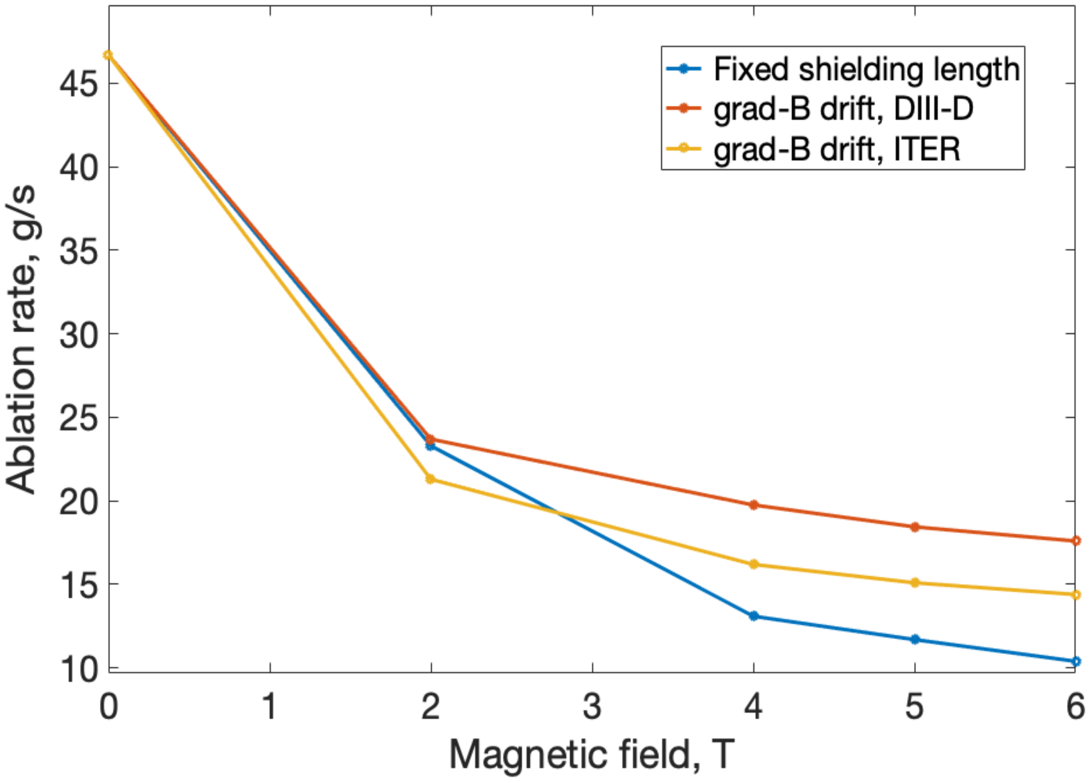

B (T) DIII-D	Shielding length, cm	G(LP, g/s)
2	18	23.7
4	14	19.76
5	13	18.45
6	12	17.6

B (T) ITER	Shielding length, cm	G(LP, g/s)
2	35.5	21.3
4	30	16.2
5	27.5	15.1
6	25.5	14.4

Weaker reduction of the ablation rate in magnetic field in simulations with grad-B drift compared to simulations with fixed shielding length. Grad-B drift effect in DIII-D is stronger compared to ITER.

Reduction of the ablation rate in magnetic field for deuterium fueling pellets: fixed shielding length compared to self-consistent shielding length

B (T) DIII-D	Shielding length	G(LP, g/s)
1.6	30 cm	35.2
2	27 cm	33.4
4	17 cm	29.7
6	15 cm	27.5

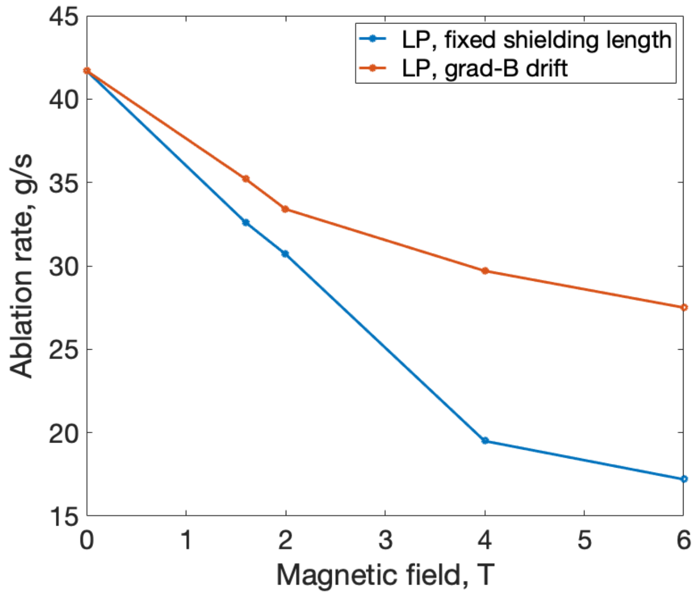

- With grad-B drift, we observe weaker reduction of the ablation rate in magnetic field compared to simulations with fixed shielding length
  - This is due to a combine effect of shorter shielding lengths and slightly changed hydrodynamic states in the ablation cloud
  - Grad-B drift in DIII-D (R_0 = 1.6 m) is stronger compared to ITER (R_0 = 6.2 m), all other factors assumed equal
  - The ablation rate of 35.2 is within 10% of the experimentally measured value (39 g/s)

- Any empirical G(B) fitting functions should be aware of the tokamak major radius
- A pellet ablation database is being built for a wide range of plasma and pellet parameters assuming a constant ratio B/R=1
- Current work in progress:
  - Fully resolved SPI simulations
  - Multiscale coupling of Lagrangian particle code with NIMROD and M3D-C1

- Runaway electrons heat the pellet volumetrically
- The threshold RE current for pellet sublimation at the edge of the RE beam is

$$j_{RE\,sb} \equiv \frac{|e|c}{2\pi r_e^2 \delta_p \ln\Lambda_{free} Z_p} \frac{\varepsilon_s}{m_e c^2} \frac{v_p}{c}$$

Pellet material	D_2	Ne	Ar
$j_{RE\,sb}$ [A/cm^2]	0.8	0.3	0.6

<<

In ITER

$j_{RE} \approx 50\,[\mathrm{A/cm^2}]$

$j_{RE\,sb}$ is very low compared to the typical current densities in tokamaks

The pellet will sublimate immediately when the RE carry a large fraction of the current

*Nuclear Fusion **60,** 084004 (2020): https://doi.org/10.1088/1741-4326/ab966a

The sublimated pellet expands rapidly as a neutral gas heated by RE

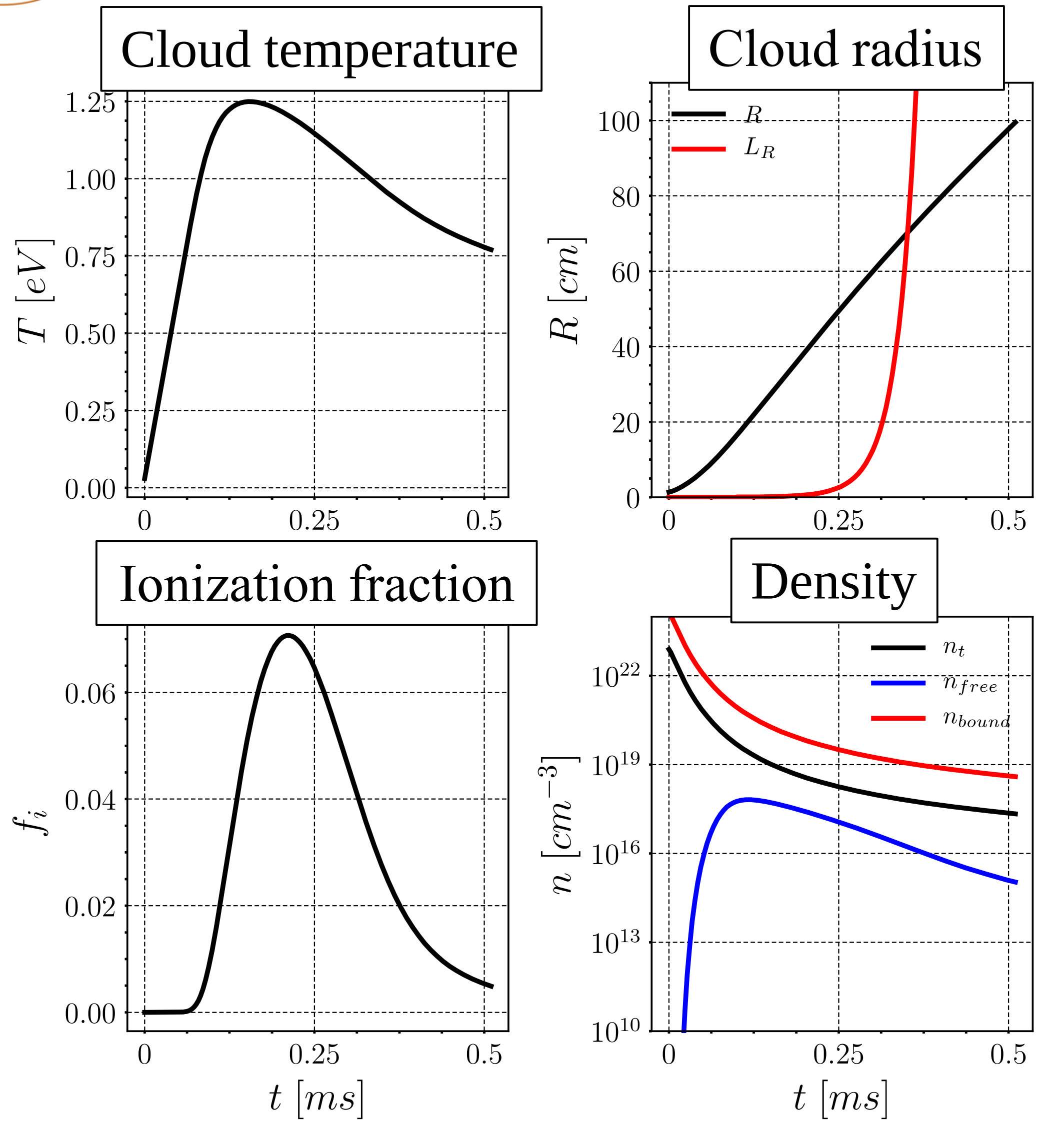

- The gas cloud spreads over the poloidal cross-section on a millisecond time scale. By the time it covers the poloidal cross-section, its temperature is in a 1 eV range, and the ionization fraction stays low

- The presented estimates explain recent experiments by D. Shiraki et al., Nucl. Fusion 58, 056006 (2018)

Net particle assimilation is generally well described by global energy balance

Empirical scalings based on pre-SPI parameters (DIII-D)

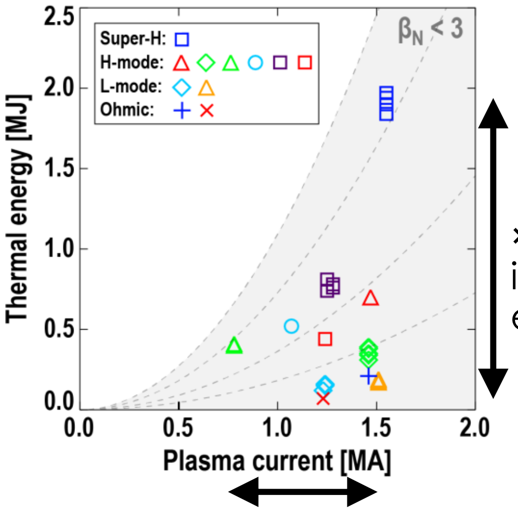

×20 change in thermal energy

×4 change in magnetic energy

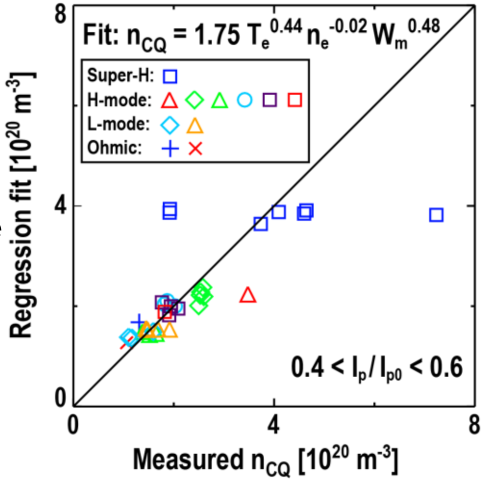

KPRAD modeling (KSTAR, DIII-D, JET)

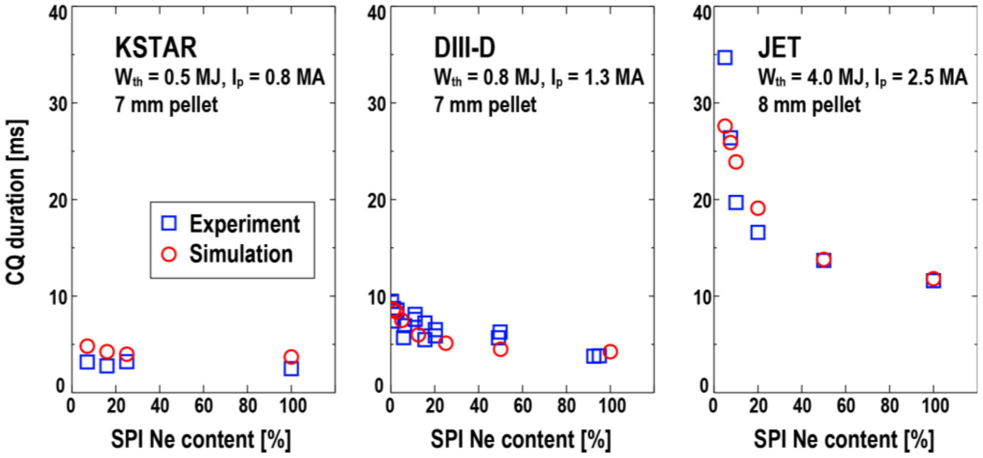

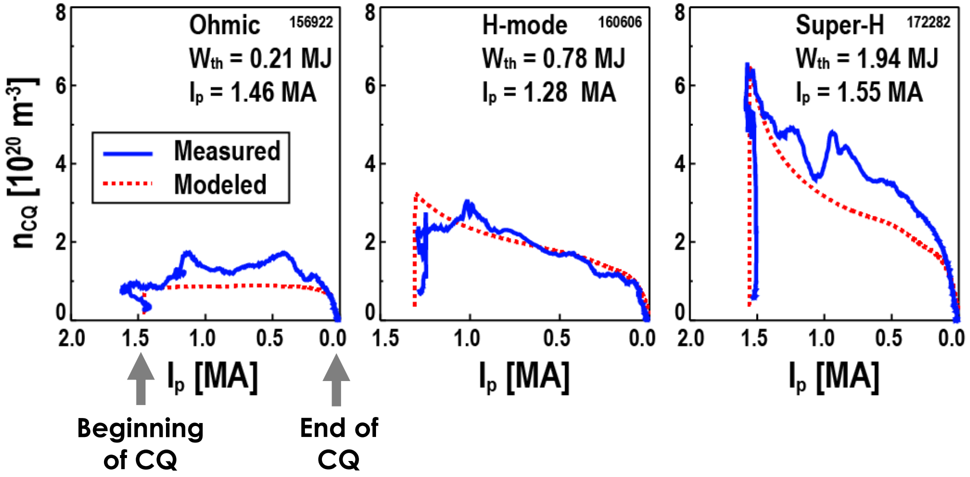

Dual-SPI results can be explained by global energy balance model, but D_2 assimilation cannot

Dual-SPI results are well captured by KPRAD

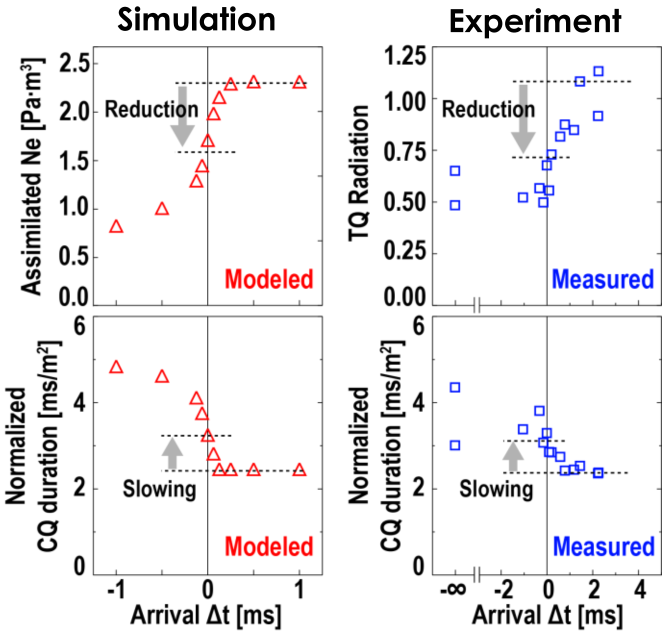

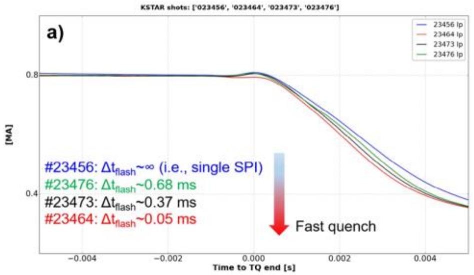

Experiment

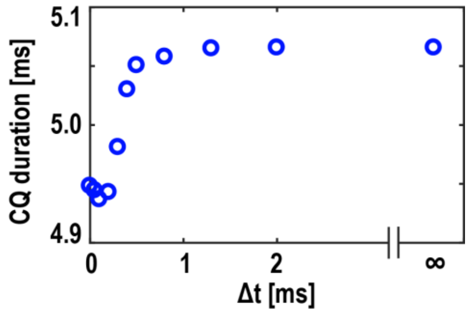

Simulation

D_2 SPI in DIII-D cannot be modeled without more complete physics

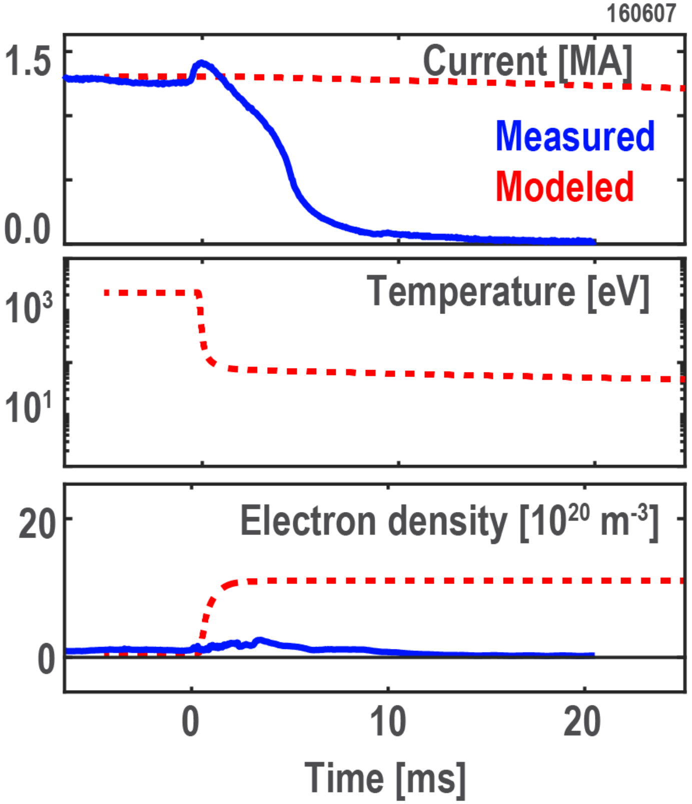

Argon SPI as trigger injection :

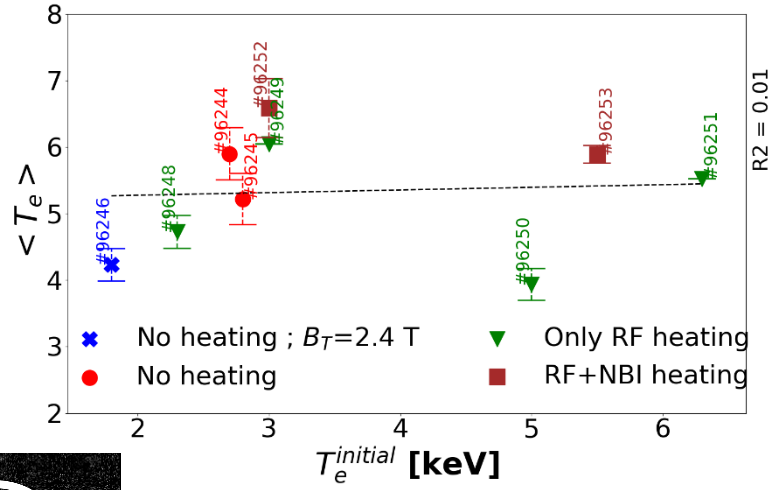

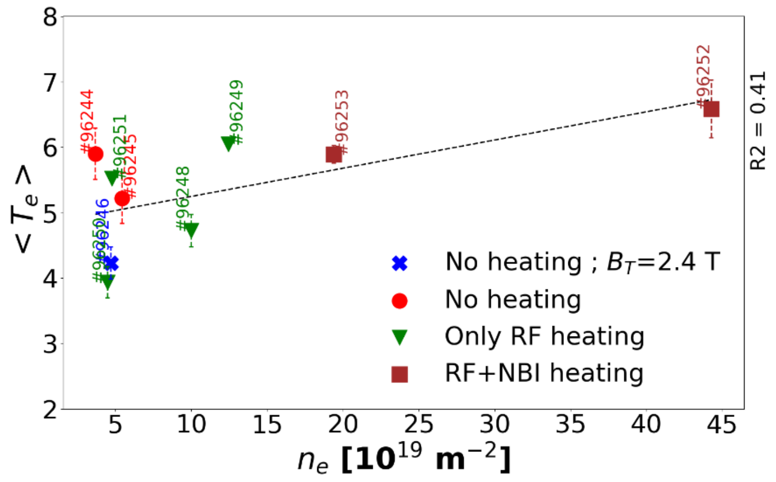

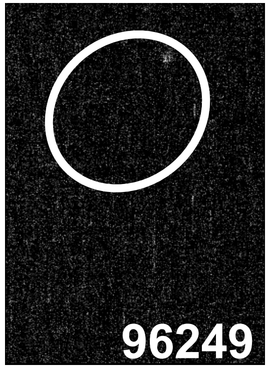

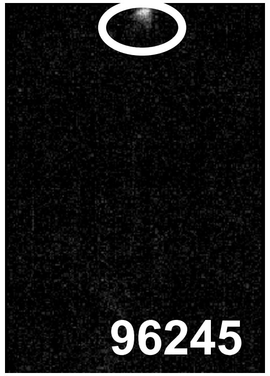

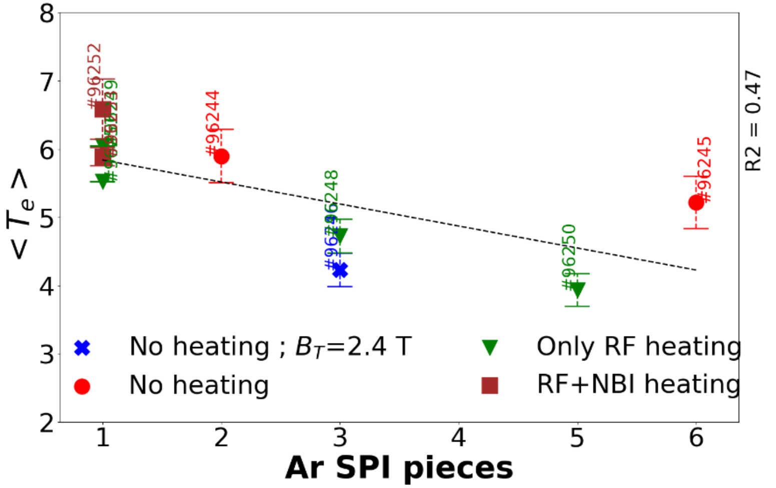

T_e of BG plasma is :

- Independent of initial T_e
- Increases with initial n_e
- Higher for intact pellets than the broken pellets ➔ better penetration of intact pellets

<Te> is estimated from VUV Spectroscopy [Sridhar et al 2020 *Nucl. Fusion*]

Ar SPI as killer injection :

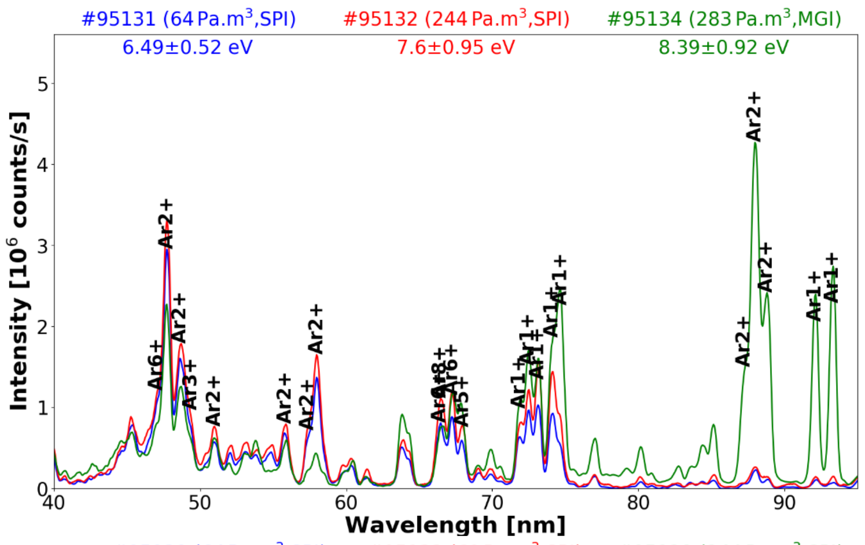

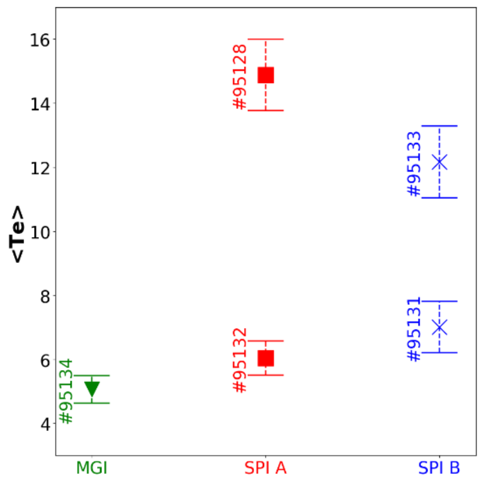

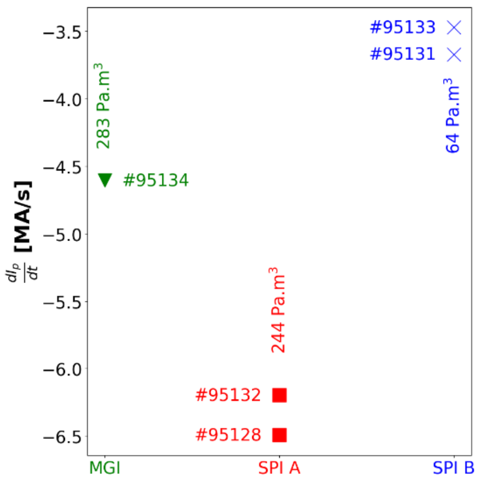

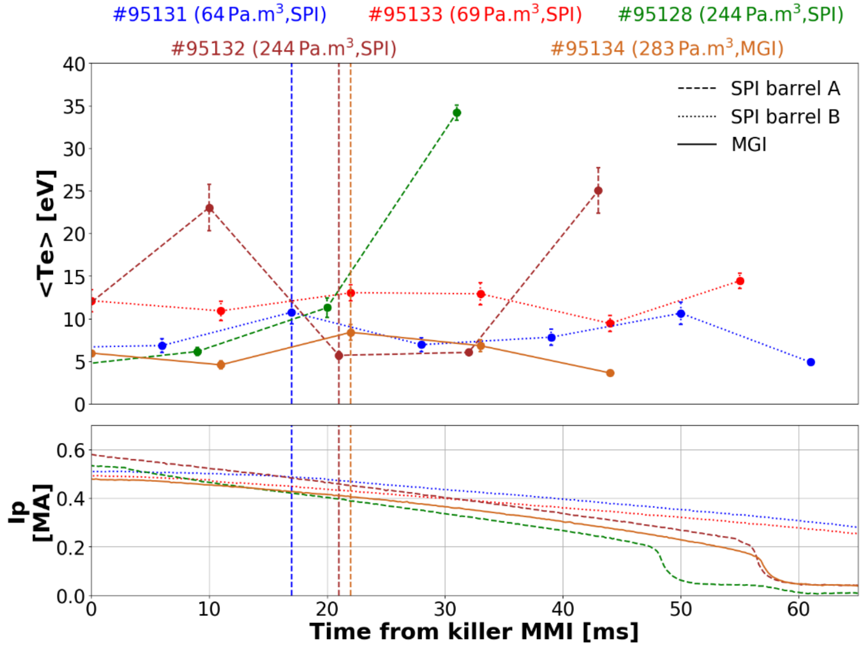

- Difference between different SPI pellets and MGI only at higher wavelength (85-100 nm)
- No clear difference in BG plasma temperature for different SPI pellets and MGI
- SPI pellet A seems to decay plasma current faster than MGI and SPI pellet B

Diffusion model :
Deuterium SPI in Ar background plasma

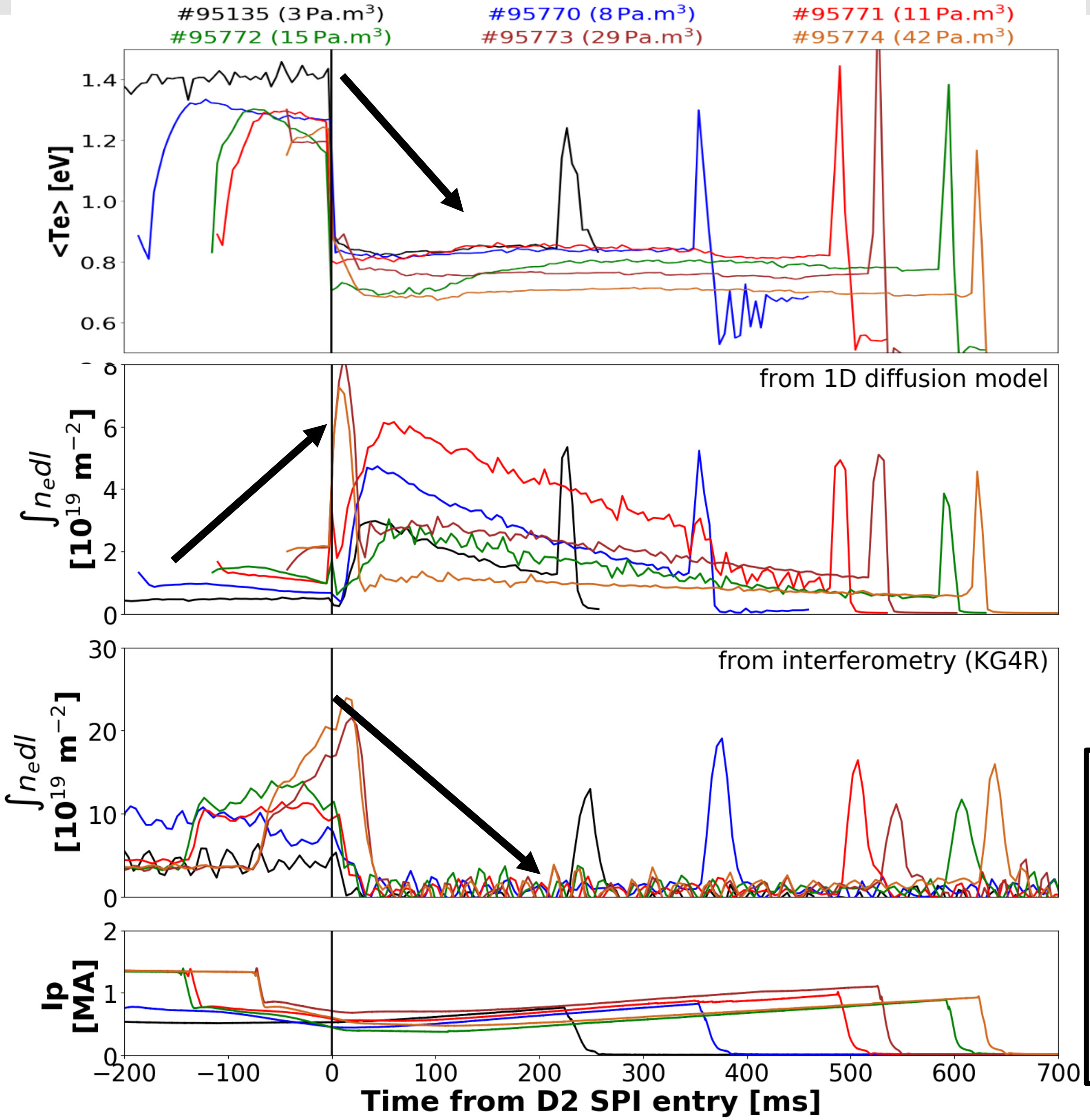

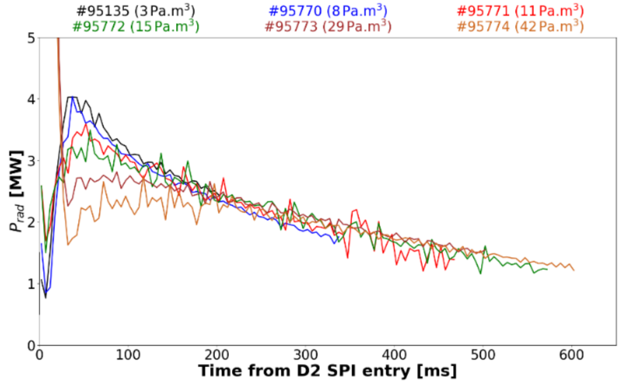

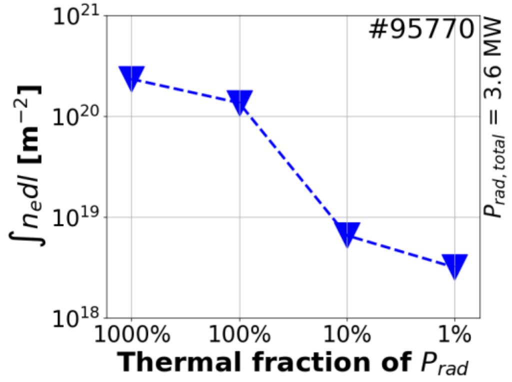

More information given by C. Reux

Diffusion model predicts :

- Te drop
- ne increase (overestimation) ➔ may be due to the omitting of non-thermal radiation in the radiated power ?

1D diffusion model from E.M. Hollmann et al 2019 Nucl. Fusion 59 106014. Thanks to Eric Hollmann for sharing the code

Summary and Perspectives

- ➢ Ar SPI as trigger injection :
  - No effect of initial T_e on VUV spectra and T_e estimation
  - T_e of BG plasma seems to increase with initial n_e ➔ similar to MGI
  - Intact pellet seems to have better penetration and hotter BG plasma

- ➢ Ar SPI as killer injection :
  - Ar SPI pellet A seems to reach higher <T_e> however no clear trend was observed
  - Ar SPI pellet A seems to decay plasma current faster than MGI and pellet B

- ➢ D_2 SPI in Ar BG plasma :
  - After D_2 SPI entry, Ar line brightness drops and deuterium lines dominates the VUV spectra

- ➢ Diffusion model :
  - T_e drops significantly after D_2 SPI injection
  - Overestimation of n_e may be due to omission of non-thermal radiation in P_{rad}
  - Model can correctly predict the drop in Ar brightness
  - ADAS data seems to predict hotter and denser BG plasma than CRETIN

  ➔ PrismSPECT atomic data also consider non-thermal radiation in cooling rate